

Laser-induced selective nitration of three cycloalkanes

Ann E. Stanley ^{*}, Judith M. Bonicamp ¹, Susan E. Godbey ², Larry M. Ludwick ³

Weapons Sciences Directorate, AMSMI-RD-WS-CM Research, Development, and Engineering Center, US Army Missile Command, Redstone Arsenal, AL 35898-5248, USA

Received 21 February 1995; accepted 24 May 1995

Abstract

Nitrated compounds are used as explosives and propellants. Laser-induced chemistry possesses the potential to drive some reactions in an efficient and selective manner, and may be useful in driving nitration reactions toward specific products. The results of several successful attempts to laser induce the reactions of nitrogen oxides with three cycloalkanes are reported. Specifically, the tunable, continuous-wave carbon dioxide infrared laser was used to drive the reaction between nitrogen dioxide and cyclopropane, cyclobutane and cyclopentane under a variety of reaction conditions. The optimization analysis of the reaction conditions is presented. In addition to the formation of nitrocycloalkanes, the other products formed were either from ring cleavage or from nitration or oxidation of ring fragments. By examining the impact of various reaction conditions on the product arrays, it was possible to find optimum conditions for producing the nitrocycloalkanes while minimizing side products.

Keywords: Laser; Infrared; Nitration; Cycloalkanes

1. Introduction

Nitrogen-containing compounds are commonly used as propellants and explosives. The chemical and physical properties of these high-energy formulations are governed by the molecular structures of the individual components. Improved methods of nitration are sought that will allow the molecular structures of the products to be selectively designed. Laser-induced chemistry is an excellent tool for this type of work.

As in the thermally driven, vapor-phase nitration [1] of cyclopropane, the laser-induced reaction of nitrogen dioxide with cyclopropane, cyclobutane and cyclopentane very likely involves the replacement of hydrogen atoms by nitro groups. It is a bimolecular reaction of the cycloalkane and nitrogen dioxide which results in the formation of nitro compounds and some alcohols. There are reactions which compete, such as the thermal isomerization of cyclopropane to propene, or, stated generally, the thermal isomerization of the cycloalkane to alkenes.

In the thermal vapor-phase nitration of cyclopropane, it was found that above 390 °C, decomposition and oxidation

of reaction mixtures occurred [1]. At lower temperatures, 335–390 °C, and longer exposure times, the thermal isomerization, oxidation and decomposition of the reaction mixture were minimized [1]. It is highly likely that a laser-induced process can be optimized with higher yield of the desired products.

Previously, we reported the successful nitration of several open-chain alkanes by nitrogen dioxide (NO₂) using a tunable, continuous-wave (CW) CO₂ laser to drive the reactions [2]. Both the yields of nitroalkanes and the selectivity of the process were promising. Subsequently, the CW CO₂ laser-induced nitration process was extended to a series of cyclic hydrocarbons, namely cyclopropane, cyclobutane and cyclopentane [3,4]. The products in these reactions were identified using gas chromatography–mass spectrometry (GC/MS) and infrared analyses. Under certain conditions, nitrocycloalkanes could be formed without making significant amounts of other nitrated products. In this paper, the nitration of the cycloalkanes is reported with a focus on the quantitative dependence of the yield of the nitrocycloalkanes in the product mixtures with respect to changes in the pressures of reactants and other laser-induced process parameters, including the usefulness of the photochemical sensitizer sulfur hexafluoride (SF₆). The objective of this project was the optimization of the yields of the nitrocycloalkanes while minimizing, if not eliminating, side products. The experiments were

^{*} Corresponding author.

¹ Permanent address: Department of Chemistry and Physics, Middle Tennessee State University, Murfreesboro, TN 37132, USA.

² Permanent address: Department of Chemistry, Eastern Kentucky University, Richmond, KY 40475, USA.

³ Permanent address: Tuskegee University, Tuskegee, AL 36088, USA.

designed with this objective in mind; however, we also followed the formation of a number of side products. This discussion includes an evaluation of the synthetic utility and specificity of the laser-driven nitration process based on all available process information.

The nitrocycloalkane products formed all have strong infrared absorption bands which are readily accessible to the output of the carbon dioxide laser. One concern is whether the nitrated products might decompose as formed or by collisional transfer, in a manner similar to the shock-initiated pyrolysis studies of nitrocyclopropane [5]. The major product of the pyrolysis study was ethene. However, theoretical studies [6] indicate that the nitro group is electron withdrawing, hence the cyclopropyl group in the nitrocyclopropane ring is stabilized by the nitro moiety.

2. Experimental section

Samples of cyclopropane, cyclopentane, 2,2-dimethylbutane, nitromethane, nitroethane, 1-nitropropane, 2-nitropropane, 2-methyl-2-nitropropane, 1-nitrobutane, 1-nitropentane, nitrocyclopentane and nitrogen dioxide were obtained from Aldrich Chemical (Milwaukee, WI, USA). The samples were of 98% or greater purity, except for 2-nitropropane (94%) and cyclopropane (95%). The cyclobutane sample was provided by Dr. S. McManus (Department of Chemistry, University of Alabama at Huntsville, AL, USA). The purity of all samples was monitored by GC/MS analysis and comparison of infrared spectra with literature spectra where available [7–12]. No further purification of the compounds was undertaken, except for nitrogen dioxide and cyclobutane, which were purified by trap-to-trap separation at -78.5°C . Nitrocyclopropane was prepared by the method of Gilkut and Borden [13]. After distillation, the sample identity was verified by NMR analysis, courtesy of the University of Alabama at Huntsville. All compounds were degassed at -196.8°C .

A stainless-steel reaction cell of exterior dimensions $5 \times 5 \times 10 \text{ cm}^3$ was used for irradiation of the reactants and subsequent analysis. This cell was equipped with either zinc selenide or potassium chloride windows on the long path through which the laser beam was directed, and AMTIR-1 windows on the short path for collecting the infrared spectra of reactants and products. The optical path lengths were 10.5 cm for the long path and 5 cm for the short path. Initial sample pressures were measured with an MKS Baratron electronic manometer, consisting of a Type 222B transducer and a Type PDR-5B power supply/digital readout. All nitration reactions followed the same general procedure. After evacuating the system to baseline pressure, the gas for the lowest pressure was admitted to the cell. Following removal of the gas from the vacuum line, the next higher pressure gas was admitted at a pressure greater than the final pressure desired. The cell valve was opened for 1–2 s to allow pressure equilibration and then closed. The gas in the vacuum system was then removed and, if necessary, a third gas component was intro-

duced into the cell in the same manner. Using this technique, a given gas mixture was reproduced readily. The reproducibility was established by monitoring the infrared absorbances of the components in the mixtures.

The infrared spectra were recorded on a Bomem DA3.002 interferometer equipped with a vacuum bench and either a deuterated TGS detector or a liquid nitrogen-cooled MCT detector and a KBr beamsplitter. The effective resolution was 1 cm^{-1} and 32 scans were recorded for both sample and reference. A medium apodization function was used [14]. Infrared spectra were recorded for reaction mixtures before and after irradiation. The infrared spectra recorded before irradiation were used to monitor the reproducibility of the initial gas pressures. These spectra were integrated over infrared spectral regions corresponding to absorbance bands of cyclopropane ($4511.3\text{--}4500.2 \text{ cm}^{-1}$) and nitrogen oxides (N_2O_4 , $1296.0\text{--}1208.2 \text{ cm}^{-1}$; N_2O_4 and NO_2 , $778.6\text{--}665.8 \text{ cm}^{-1}$). A linear relationship between the areas and partial pressures of the reactants was observed in all cases.

A Coherent Radiation Model 41 CW CO_2 tunable laser provided the excitation energy to drive the reactions. This laser was operated in a single mode at various selected wavelengths and powers. The selected wavelength was verified using an Optical Engineering CO_2 spectrum analyzer. The laser powers were measured using a Coherent Radiation Model 213 water-cooled power meter.

The reaction cell was positioned on a movable stage which could be translated in the X and Y directions along the laser beam. All samples were irradiated with the cell positioned just behind the focal point where the beam was slightly diverging. The zinc selenide windows allowed a beam transmittance of about 70% through the sample cell. The KCl windows allowed about 86% of the beam through the two windows to the power meter. The reported laser powers do not correct for this window absorption or for the difference in beam diameter at the sample, as opposed to the diameter at the power meter. The beam diameter was approximately 2 mm at the point of entry to the reaction cell.

The separation and analysis of the reaction products were accomplished using a Hewlett-Packard (HP) model 5890 gas chromatograph equipped with a 0.250 ml gas sampling loop and interfaced to an HP 5970 series mass-selective detector. The chromatographic column was a $40 \text{ m} \times 0.2 \text{ mm}$ i.d. HP Ultra 2 (crosslinked 5% phenylmethylsilicone) with a 0.22 μm film thickness. The volumetric flow rate was $1.6 \text{ cm}^3 \text{ min}^{-1}$ (linear flow rate 10 m min^{-1}); the splitting ratio was 47:1 and the column head pressure was 10 psi. For chromatographic analysis, two different temperature programs were used. With cyclopropane, cyclobutane and some cyclopentane mixtures, the oven temperature was maintained at 40°C for 5 min, then programmed to 140°C at $10^{\circ}\text{C min}^{-1}$. For other cyclopentane reaction mixtures, the initial oven temperature was 60°C and programming to 160°C at $10^{\circ}\text{C min}^{-1}$ began immediately. Identification of the components of the chromatographic peaks was attempted using the computer search routine and the NBS43k Mass Spectra Library.

Whenever possible, component identities were verified by comparing the gas chromatographic retention times and the mass spectra with those of known samples. The separation of some highly volatile components was not possible with the chromatographic conditions used.

Irradiation of the cyclopentane reaction mixtures frequently produced visible condensation of liquid on the KCl windows. A procedure was developed to determine the amount of liquid formed. Following the removal of a gas sample to the gas sampling loop, the cell was opened and 2.0 ml of absolute ethanol were added using a 10.00 ml pipet. After rinsing the inside of the cell for 5–10 min, the ethanol solution was removed and placed in a septum-sealed vial. Following each ethanol wash, the KCl cell windows were polished to remove cloudiness. Liquid samples (0.5 μl) of the wash solution were injected into the GC/MS system using a 1.0 μl syringe. Several injections were averaged to give GC/MS total ion areas for nitrocyclopentane, the only nitroalkane identified in the ethanol solution. A calibration graph from the GC/MS total ion areas of a series of standard solutions of nitrocyclopentane in absolute ethanol was used to quantify the nitrocyclopentane produced in the reaction. A calibration graph was constructed as follows: volumes of neat nitrocyclopentane (1.0–8.0 μl) were added to the empty reaction cell, 2.0 μl of absolute ethanol were added, the solution was mixed by swirling and then 0.50 ml samples of the "cell wash" were injected into the GC/MS system using the same chromatographic techniques as was used for samples. Total ion counts were plotted vs. volume of nitrocyclopentane (μl) per 2.0 ml of solution.

The program XYMATH (C. Taylor, P.O. Box 277875, Sacramento, CA 95827-7875, USA) was used for curve-fitting of the GC/MS total ion areas and the infrared spectral integrals. All lines presented in the figures were generated empirically using best-fit modeling from XYMATH. All lines presented represent statistically significant relationships.

3. Results and discussion

The CW carbon dioxide infrared laser emits several intense bands of radiation in the frequency region between 900 and 1100 cm^{-1} . Absorbance spectra for the three cycloalkanes [3] reveal vibrational bands for each compound that are accessible by the output of the CO_2 laser. These bands indicate why it was possible to initiate and sustain by laser excitation the reaction of the hydrocarbons with nitrogen dioxide. In instances where the power output of the laser transition is low or the hydrocarbon absorption is weak at that frequency, an infrared sensitizer, sulfur hexafluoride, was used to initiate the reaction indirectly.

Mixtures of each cyclic hydrocarbon with nitrogen dioxide were irradiated under variable conditions of laser powers, irradiation frequencies and times and pressures of reactants or sensitizer. For each hydrocarbon, results are presented which illustrate the statistically significant impact of varying

the conditions on the relative amounts of products formed. The relationships which are presented in the figures and discussed are generated using XYMATH best-fit mathematical analysis. The correlation coefficients were very high in all cases.

3.1. Cyclopropane

Cyclopropane has two infrared absorption bands which are accessible to the output frequencies of the CO_2 laser, at 866 and 1027 cm^{-1} . Although not on the absorption maximum, the CO_2 laser output from the P(18) line of the $(00^01)-(02^00)$ transition at 1048.7 cm^{-1} could be varied easily from 20 to 50 W cm^{-2} , which was one reason that this line was chosen for irradiation of cyclopropane mixtures. Other CO_2 output lines were not only on the periphery of the absorption band of cyclopropane, but also afforded limited laser power output.

When mixtures of cyclopropane and nitrogen oxides were irradiated, the quantity of nitrogen oxides consumed depended on the initial pressure of cyclopropane, as determined by infrared spectral analysis. Typical infrared spectra are shown in Fig. 1 and typical chromatograms in Fig. 2. Fig.

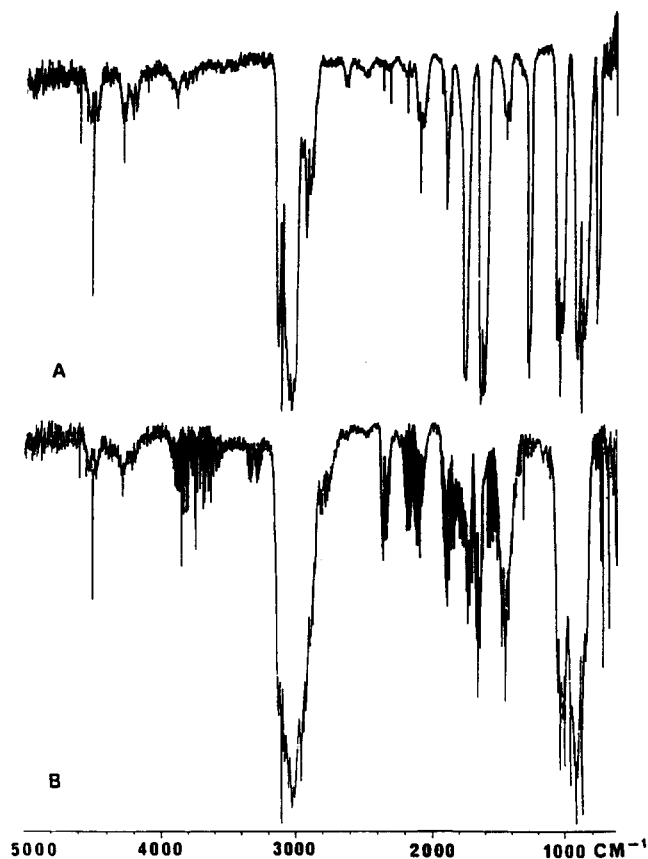


Fig. 1. Gas-phase mid-infrared spectra of cyclopropane– NO_2 mixture before excitation and products resulting from the CO_2 laser excitation of the mixture: (A) spectrum of cyclopropane (170.4 Torr) and NO_2 (30.0 Torr); (B) spectrum of products formed from the CO_2 laser excitation of the mixture in (A) under the conditions P(18) of $(00^01)-(02^00)$, 1048.7 cm^{-1} , 50 W cm^{-2} , 20 s.

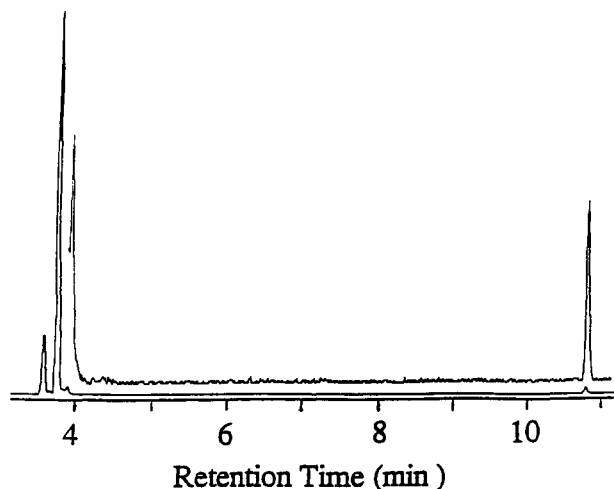


Fig. 2. Gas chromatogram from the analysis of the product mixture from the CO_2 laser excitation of 191.1 Torr of cyclopropane and 40.0 Torr of NO_2 for 60 s at 30 W cm^{-2} laser power on the P(18) line of the $(00^01)-(02^00)$ transition (1048.7 cm^{-1}).

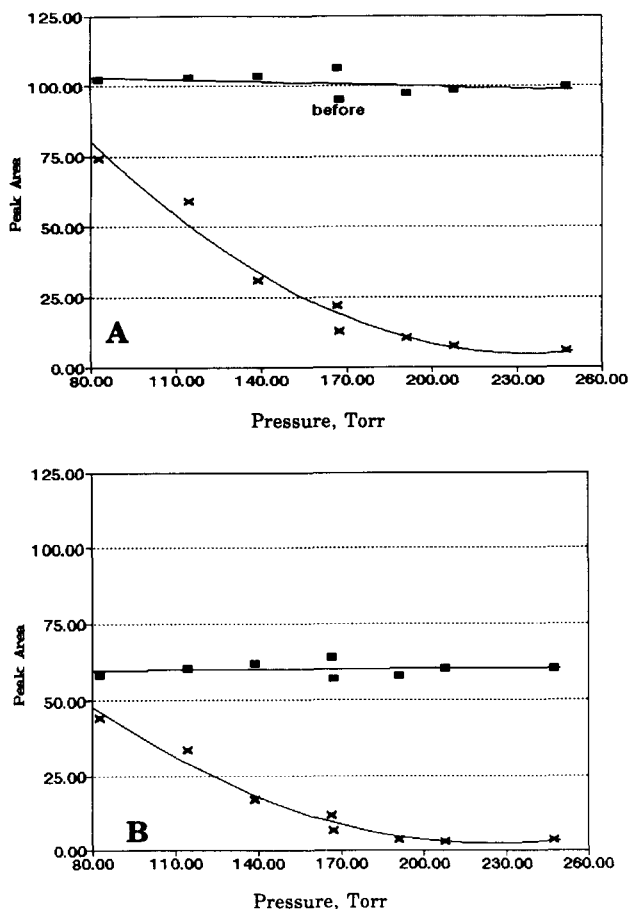


Fig. 3. Nitrogen oxides (40 Torr) versus cyclopropane pressure before and after irradiation for 60 s at 30 W cm^{-2} using the P(18) line of the $(00^01)-(02^00)$ transition, 1048.7 cm^{-1} : (A) N_2O_4 infrared peak areas; (B) $\text{N}_2\text{O}_4 + \text{NO}_2$ infrared peak areas.

3 shows the depletion of nitrogen oxides (40 Torr) when the mixtures were irradiated at 30 W cm^{-2} for 60 s. The amount of cyclopropane used during irradiation with nitrogen oxide

mixtures showed a dependence on the initial pressure of cyclopropane. Irradiation products identified from the infrared spectra include H_2O , HCN (traces in a few samples), CO_2 , NNO, CO, NO, formic acid, ethene and nitrocyclopropane [3]. The frequency regions over which integrals were acquired are given in Table 1. Fig. 4 shows the manner in which the formation of nitrocyclopropane depended on the initial pressure of cyclopropane, as determined by both gas-phase infrared analysis and GC/MS analysis using the gas sampling loop. At a constant nitrogen oxides pressure of 40

Table 1
Infrared frequency regions for integrals of reactants and products in the cyclopropane and nitrogen oxides systems

Frequency interval (cm^{-1})	Identity
4511.3–4500.2	Cyclopropane
1390.9–1349.0	Nitrocyclopropane
1296.0–1208.2	N_2O_4
952.1–943.5	Ethene
778.6–720.3	$\text{N}_2\text{O}_4 + \text{NO}_2$

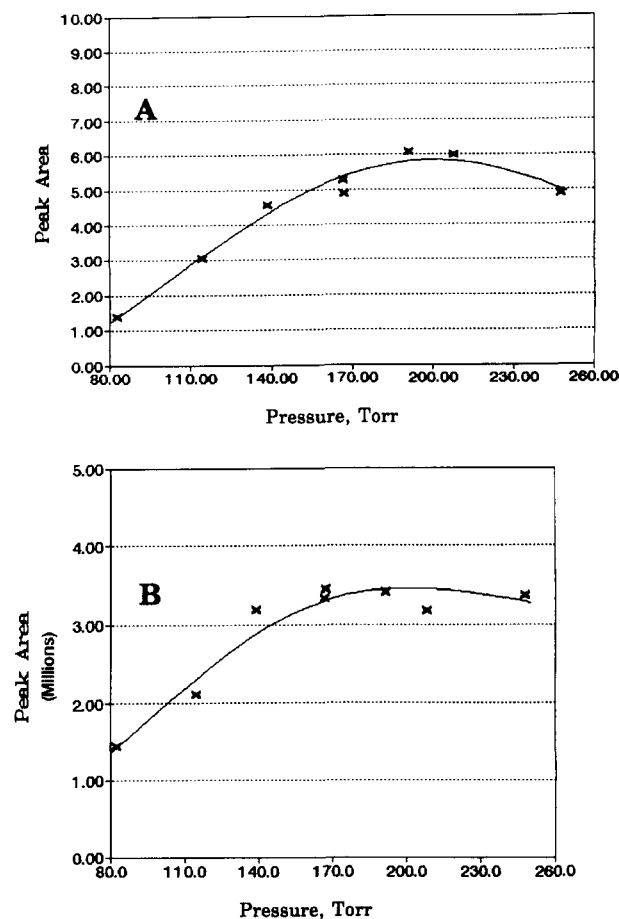


Fig. 4. Nitrocyclopropane production versus cyclopropane pressure after irradiation of mixtures containing 40 Torr of nitrogen oxides for 60 s at 30 W cm^{-2} using the P(18) line of the $(00^01)-(02^00)$ transition, 1048.7 cm^{-1} : (A) nitrocyclopropane infrared peak areas; (B) nitrocyclopropane GC/MS peak areas.

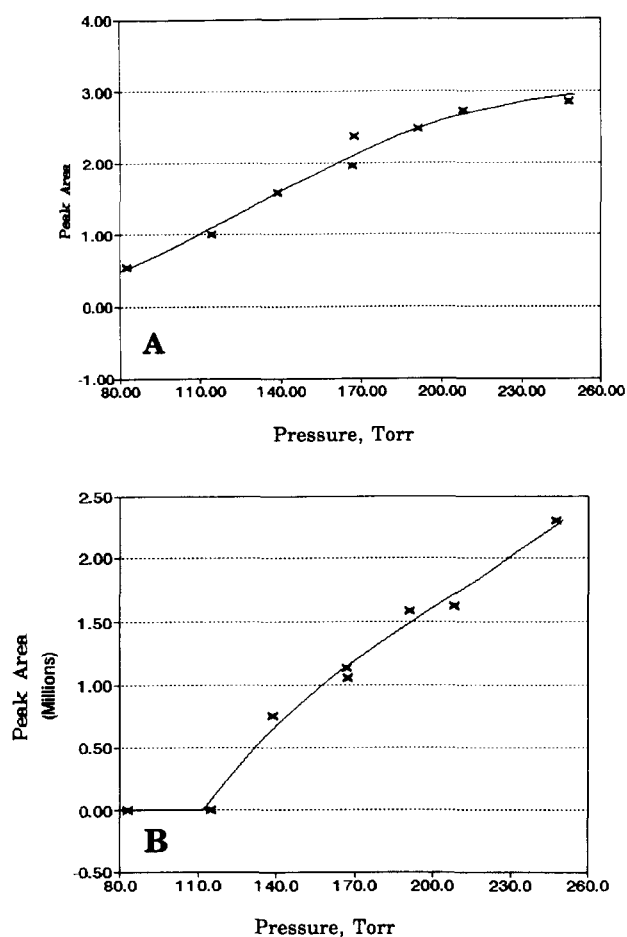


Fig. 5. (A) Ethene production versus cyclopropane pressure: ethene infrared peak areas after irradiation of mixtures containing 40 Torr of nitrogen oxides for 60 s at 30 W cm^{-2} using the P(18) line of the $(00^{\circ}1)-(02^{\circ}0)$ transition, 1048.7 cm^{-1} . (B) Propene production versus cyclopropane pressure: propene GC/MS peak areas after irradiation of mixtures containing 40 Torr of nitrogen oxides for 60 s at 30 W cm^{-2} using the P(18) line of the $(00^{\circ}1)-(02^{\circ}0)$ transition, 1048.7 cm^{-1} .

Torr, the yield of nitrocyclopropane in the vapor phase of the product mixture increased up to a pressure of about 200 Torr of cyclopropane. Beyond this pressure, if more nitrocyclopropane was produced it was in the condensed phase and was not detected by infrared or GC/MS analysis. The only nitroalkane produced under these conditions was nitrocyclopropane. The other products present were either from ring cleavage or from nitration or oxidation of ring fragments. All of the ring-cleavage products showed a strong dependence on the partial pressure of cyclopropane, with the production of formic acid, ethene [see Fig. 5(A)] and carbon dioxide leveling off as the cyclopropane pressure increased. Production of hydrogen cyanide and the fragment CO also increased as the cyclopropane pressure rose. Increasing the cyclopropane pressure also resulted in more NO and NNO. The GC/MS analysis of some product mixtures revealed the presence of propene [see Fig. 5(B)], 2-propenal and acetonitrile, in addition to a large mixed gas peak. The mixed gas peak resulted from both water and those highly volatile components not separable with the chromatographic conditions used. The production of mixed

gases increased as the pressure of cyclopropane increased. The product propene did not appear in the GC/MS traces until the cyclopropane pressure in the reaction mixtures was greater than about 120 Torr.

The infrared integrals and the GC/MS total ion areas allowed the evaluation of the impact on product formation of varying nitrogen oxide pressures at a constant partial pressure of cyclopropane of 200 Torr. When mixtures were irradiated at 30 W cm^{-2} for 30 s, the amount of cyclopropane remaining in the product mixtures decreased as the nitrogen oxide pressure in the reaction mixtures increased (Fig. 6). Similarly, the greater the nitrogen oxides pressure initially, the more the nitrogen oxides were consumed. The specific amount of nitrogen oxides remaining after irradiation was difficult to determine using infrared integrals. Because the nitrogen oxides participate in complex, temperature-dependent equilibria, their infrared integrals are sensitive to small variations in cell temperature. The ring-cleavage products, ethene [see Fig. 7(A)], HCN, formic acid, CO_2 and CO increased in a near-linear manner with increasing pressure of nitrogen oxides, as did the product NO and the mixed gas peak in the GC/MS analyses. Increasing the nitrogen oxides pressure did not increase the nitrocyclopropane produced unless the product condensed on the cell walls. The infrared and GC/MS anal-

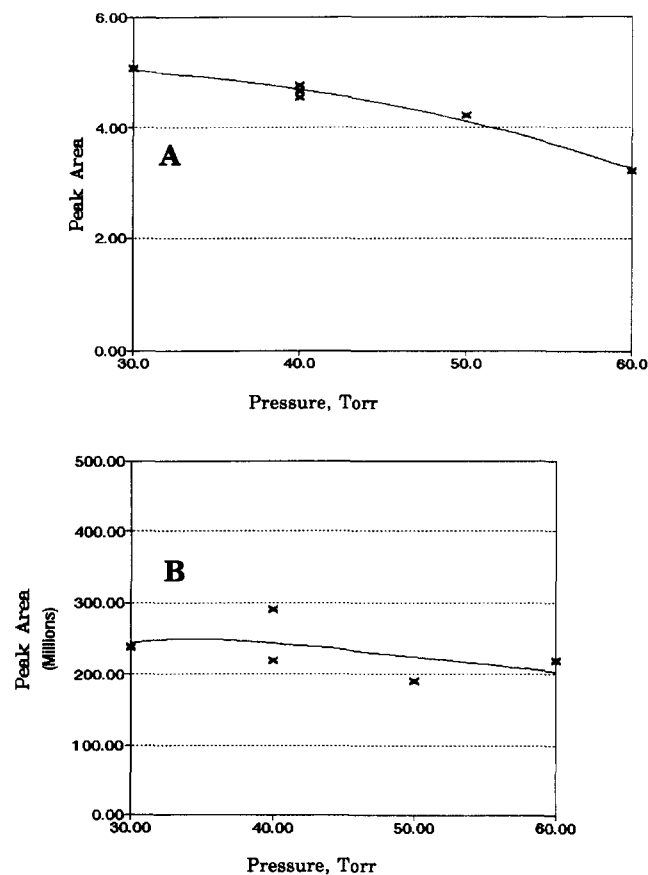


Fig. 6. Cyclopropane (200 Torr) depletion versus nitrogen oxides pressure after irradiation for 30 s at 30 W cm^{-2} using the P(18) line of the $(00^{\circ}1)-(02^{\circ}0)$ transition, 1048.7 cm^{-1} : (A) cyclopropane infrared peak areas; (B) cyclopropane GC/MS peak areas.

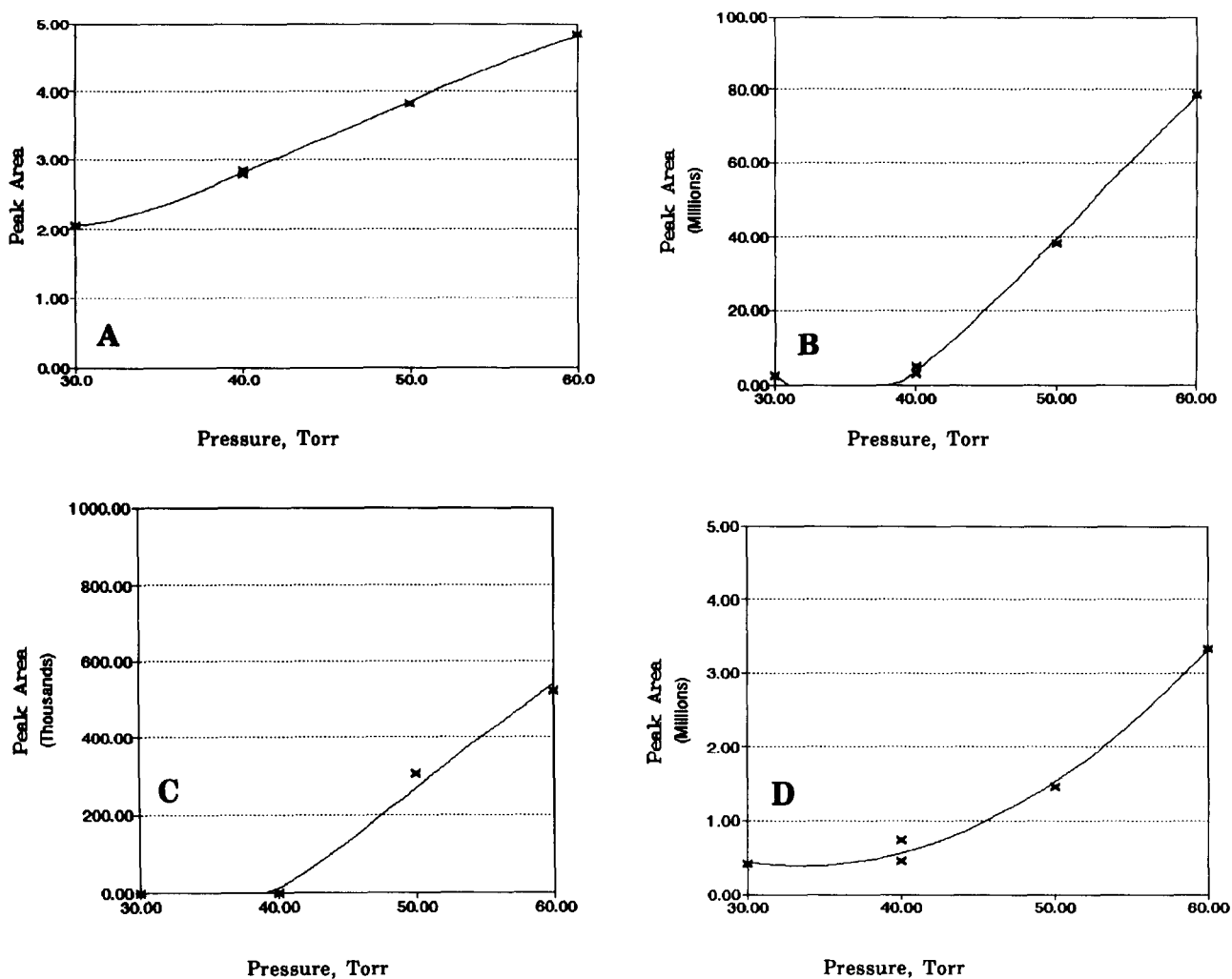


Fig. 7. (A) Ethene production versus nitrogen oxides pressure: ethene infrared peak areas after irradiation of mixtures containing 200 Torr of cyclopropane for 30 s at 30 W cm^{-2} using the P(18) line of the $(00^01)-(02^0)$ transition, 1048.7 cm^{-1} . (B) Propene gas production versus nitrogen oxides pressure: propene GC/MS peak areas after irradiation of mixtures containing 200 Torr of cyclopropane for 30 s at 30 W cm^{-2} using the P(18) line of the $(00^01)-(02^0)$ transition, 1048.7 cm^{-1} . (C) Nitromethane production versus nitrogen oxides pressure: nitromethane GC/MS peak areas after irradiation of mixtures containing 200 Torr of cyclopropane for 30 s at 30 W cm^{-2} using the P(18) line of the $(00^01)-(02^0)$ transition, 1048.7 cm^{-1} . (D) Propenal production versus nitrogen oxides pressure: propenal peak areas after irradiation of mixtures containing 200 Torr of cyclopropane for 30 s at 30 W cm^{-2} using the P(18) line of the $(00^01)-(02^0)$ transition, 1048.7 cm^{-1} .

yses of the vapor phase yielded nitrocyclopropane versus nitrogen oxide plots with the production of nitrocyclopropane almost flat as the nitrogen dioxide pressure increased from 30.0 to 60.0 Torr. The GC/MS analysis of the product mixtures occasionally revealed the presence of a number of other components, propene [Fig. 7(B)], acetonitrile, propenitrile and nitromethane, these products appearing when the nitrogen oxide pressure exceeded 40 Torr and increasing almost linearly thereafter. Nitromethane [Fig. 7(C)] was the only other nitroalkane produced from nitrogen oxide and cyclopropane mixtures. Fig. 7(D) shows a similar dependence for the production of 2-propenal, except that 2-propenal could be detected when the initial nitrogen oxide pressure was 30 Torr.

Conditions of higher laser power (50 W cm^{-2}) promoted the fragmentation of reactants and products. The infrared spectra showed additional products including methane, acet-

ylene, and formaldehyde [3]. Propene and 2-propenal now could be identified in the infrared spectrum of the product mixture, whereas in the preceding experiments these products could not be detected in the infrared spectra, although they were present in the GC/MS trace. In the 50 W cm^{-2} product mixtures, neither nitrocyclopropane nor any other nitroalkane could be detected in the infrared or in the GC/MS analyses.

A series of 30 s irradiation experiments, in which the pressures of reactant gases were held constant (cyclopropane, 212 Torr; nitrogen oxides, 50 Torr) but in which the irradiation power was varied, allowed us to assess the impact of moderate laser powers on the reaction. Fig. 8 shows the response of cyclopropane pressures to increasing irradiation power as determined from the infrared integrals and from the GC/MS total ion count. The nitrogen oxides showed a greater impact to increasing laser power and were in fact completely depleted from the product mixtures when the laser power

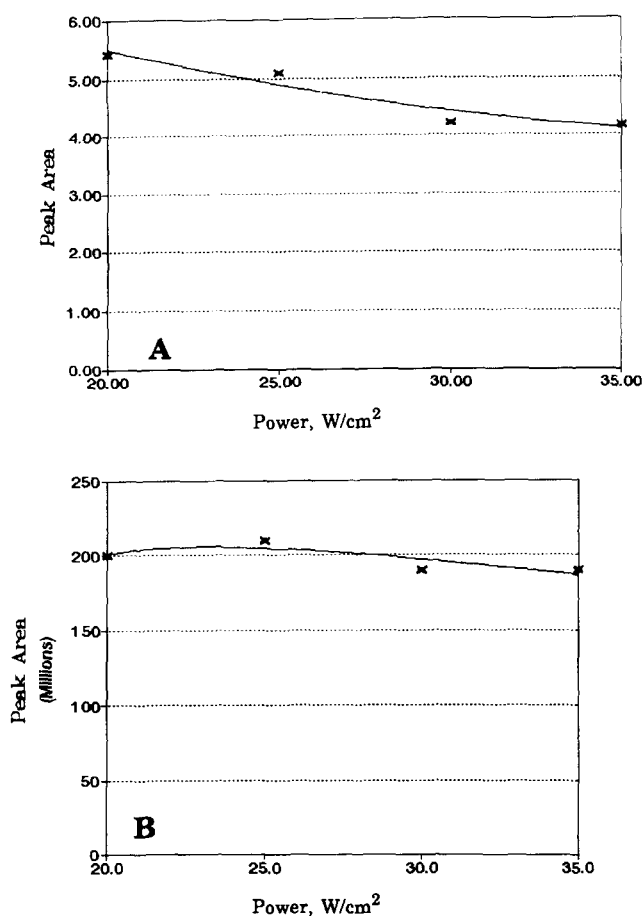


Fig. 8. Cyclopropane (212.5 Torr) remaining versus incident laser power after irradiation of mixtures containing 50 Torr of nitrogen oxides for 30 s using the P(18) line of the (00¹)-(02⁰) transition, 1048.7 cm⁻¹: (A) cyclopropane infrared peak areas; (B) cyclopropane GC/MS peak areas.

approached 35 W cm⁻² (Fig. 9). The yield of nitrocyclopropane in the gas phase reached a maximum at about 25–30 W cm⁻². The decrease in nitrocyclopropane yield above 30 W cm⁻² (Fig. 10) is consistent with an increase in the production of smaller molecules and fragmentation at higher laser powers, as described above for the 50 W cm⁻² experiments. The production of HCN, ethene [Fig. 11(A)] and formic acid increased with increasing irradiation power. The ethene and formic acid production leveled off as the power increased. Formic acid decomposition (in the product mixture) may well yield CO₂ and CO, the production of which was favored as the laser power approached 35 W cm⁻². Production of NO leveled off before 35 W cm⁻², but production of NNO continued to rise linearly with increasing irradiation power. The composition of the mixed gas peak varies with the irradiation power as infrared analysis prior to gas chromatography of the product mixtures indicates: at low laser powers the peak consists of small molecules and unreacted nitrogen oxides, but at higher powers the NO₂ and N₂O₄ are depleted, and the peak contains more of the species resulting from fragmentation and oxidation reactions, CO₂, CO, NO and NNO. Acetonitrile, propenitrile and nitromethane were not detected by GC/MS until the laser power had been raised to 30 W cm⁻²,

after which the yield rose as the power increased, with nitromethane [Fig. 11(B)] production falling again after 30 W cm⁻². Propene and 2-propenal could be detected by GC/MS at 20 and 25 W cm⁻², respectively, but their amounts remained relatively low until the power was raised above 30 W cm⁻², beyond which their production was facilitated [Fig. 11(C) and (D)].

A final set of experiments were conducted with fixed partial pressures of cyclopropane and nitrogen oxides (209 and 40 Torr, respectively) and with the laser power constant at 25 W cm⁻², to evaluate the effect of irradiation time on the product yield. The specific irradiation power was 25 W cm⁻², which was thought to be optimal for producing nitrocyclopropane. As Fig. 12 shows, the amount of cyclopropane remaining after irradiation decreased slightly at longer irradiation times; however, the amount of nitrogen oxides remaining in the reaction mixture showed no clear dependence on irradiation time. The yield of nitrocyclopropane in the vapor phase showed little increase with irradiation time over the range studied; however, a number of other products were followed as the irradiation time varied. Increasing the

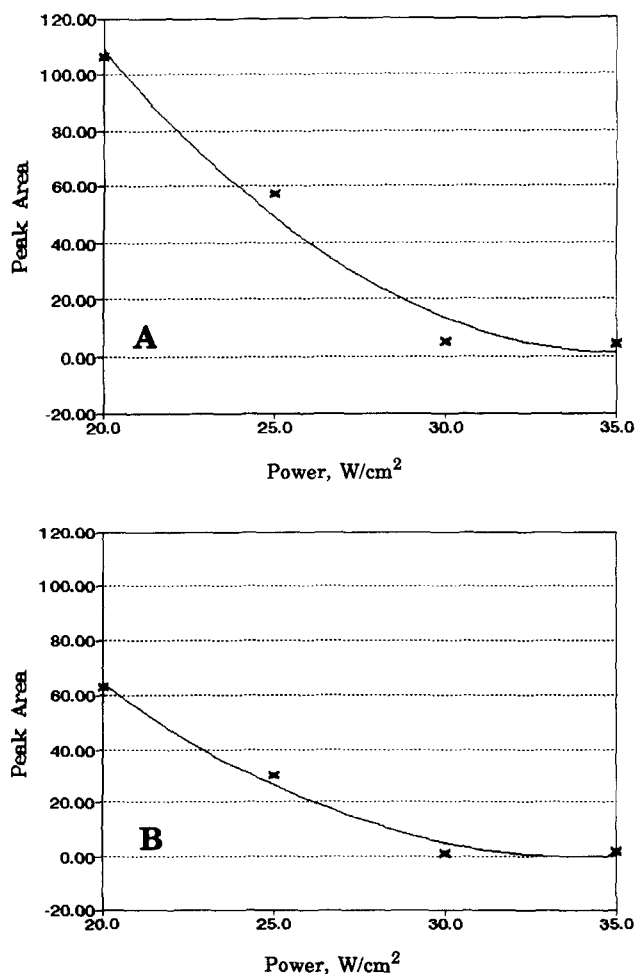


Fig. 9. Nitrogen oxides (50 Torr) remaining versus incident laser power after irradiation of mixtures containing 212.5 Torr of cyclopropane for 30 s using the P(18) line of the (00¹)-(02⁰) transition, 1048.7 cm⁻¹: (A) N₂O₄ infrared peak areas; (B) NO₂ infrared peak areas.

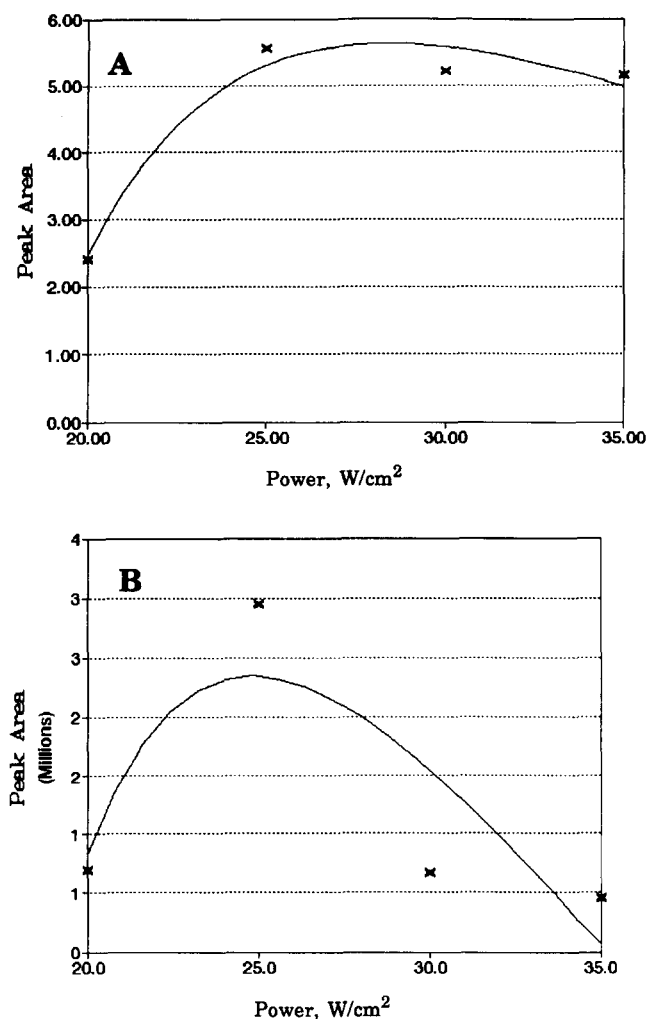


Fig. 10. Nitrocyclopropane versus incident laser power after irradiation of mixtures containing 212.5 Torr of cyclopropane and 50 Torr of nitrogen oxides for 30 s using the P(18) line of the (00⁰1)–(02⁰) transition, 1048.7 cm⁻¹: (A) nitrocyclopropane infrared peak areas; (B) nitrocyclopropane GC/MS peak areas.

irradiation time from 20 to 30 s resulted in the formation of ethene, CO₂, CO and NO; however, their yields showed little dependence on longer irradiation times. With the low laser power utilized, the quantities of formic acid, HCN and NNO produced were so small that we could not follow the time dependence of their formation. The GC/MS traces indicated that the maximum production of propene occurred at irradiation times of 20–30 s (Fig. 13), and also that the mixed gas production rose until the irradiation time was about 45 s.

By careful selection of the conditions, it is possible to produce nitrocyclopropane with no detectable amounts of any other nitrated products. A mixture of cyclopropane (191.1 Torr) and NO₂ (40.0 Torr) which had been irradiated at 30 W cm⁻² for 60 s gave nitrocyclopropane, the only nitroalkane present, at a retention time of 10.8 min; any other nitroalkanes should have appeared in the chromatogram at retention times greater than 5 min under the GC/MS conditions we employed.

3.2. Cyclobutane

The infrared spectrum of cyclobutane shows a single, weak absorption band centered at 900 cm⁻¹, which is accessible to the output of the CW carbon dioxide laser. Irradiation using the P(42) laser line of the (00⁰1)–(10⁰) transition at 922.9 cm⁻¹ was on the R branch near the maximum at 922 cm⁻¹. Because of both the weak absorption and the limited laser power available, longer irradiation times were necessary to induce the nitration reaction. Typical infrared spectra and GC/MS traces are shown in Figs. 14 and 15. Table 2 shows the frequency intervals over which integrals were acquired for both reactants and products.

Irradiation of 200 Torr of cyclobutane and 40.0 Torr of NO₂ using the P(42) line at 60 W cm⁻² for 60 s yielded products identified by infrared analysis as H₂O, CO₂, CO, NO, formic acid and ethene [3]. We have tentatively assigned the other absorbance bands at 1560 and 1376 cm⁻¹ to nitrocyclobutane. The quantity of nitrogen oxides consumed during irradiation was dependent on the pressure of cyclobutane, as Fig. 16 shows for nitrogen oxides at a starting pressure of 40 Torr. The infrared region usually integrated for N₂O₄ (1296.0–1228.0 cm⁻¹) also includes a cyclobutane absorbance band. For this reason, data for the N₂O₄ peak are not presented. The amount of cyclobutane used during irradiation did not depend appreciably on the initial pressure of cyclobutane. Nitrocyclobutane and 1-nitropropane were found in the chromatogram at 13.6 and 9.4 min, respectively. The quantity of nitrocyclobutane produced showed a near-linear relationship to the partial pressure of cyclobutane in the reaction mixtures (Fig. 17).

A similar dependence for the formation of 1-nitropropane, the only other nitroalkane identified by GC/MS analysis, is illustrated in Fig. 18(A); however, no 1-nitropropane was detected until the initial cyclobutane pressure was greater than 80 Torr. Trends for the products arising from cleavage of the cyclobutane ring are illustrated in Fig. 18(B) and (C). Formic acid, carbon dioxide and 2-butene show a similar dependence on the cyclobutane pressures in the reaction mixtures: as the cyclobutane pressure rose, the products increased then leveled off, or perhaps decreased. The production of ethene increased smoothly as the cyclobutane pressure increased. Although the fragment CO was identified in the infrared spectra, its formation was not followed owing to the presence of large cyclobutane absorbances which obscured the CO absorption bands. Nitrogen monoxide is another compound whose production appeared to level off with increasing pressure of cyclobutane. The mixed gas production as monitored from the GC/MS peak area remained fairly constant as the cyclobutane pressure varied from 40 to 200 Torr, although the composition of the peak certainly varied as more nitrogen oxides reacted and low molecular weight volatile products were formed.

A series of 60 s irradiation experiments, in which the cyclobutane pressure was 179 Torr and the nitrogen oxide pressure was 40 Torr, but with the irradiation power varied from 45

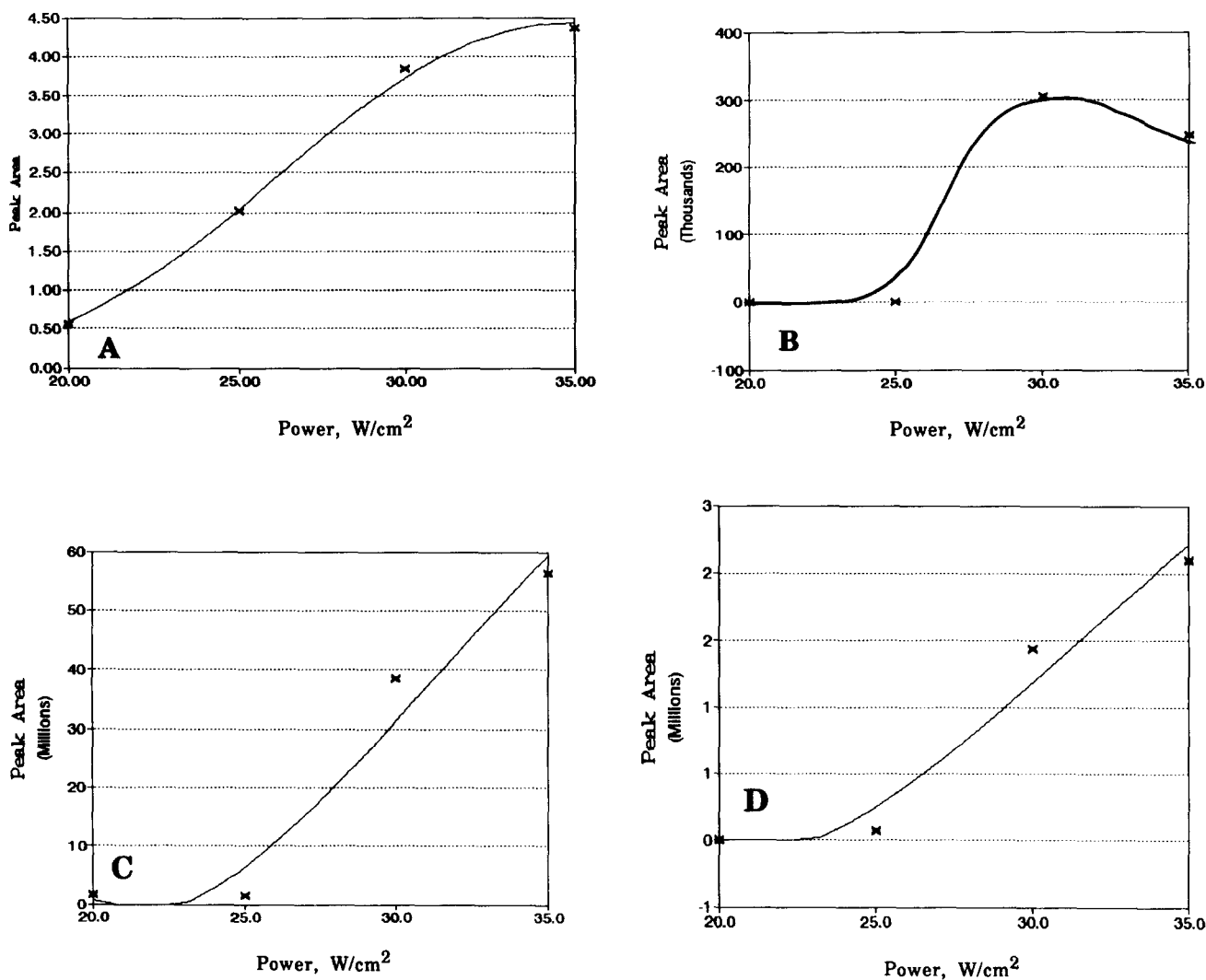


Fig. 11. (A) Ethene produced versus incident laser power: ethene infrared peak areas after irradiation of mixtures containing 212.5 Torr of cyclopropane and 50 Torr of nitrogen oxides for 30 s using the P(18) line of the (00¹)–(02⁰) transition, 1048.7 cm⁻¹. (B) Nitromethane produced versus incident laser power: nitromethane GC/MS peak areas after irradiation of mixtures containing 212.5 Torr of cyclopropane and 50 Torr of nitrogen oxides for 30 s using the P(18) line of the (00¹)–(02⁰) transition, 1048.7 cm⁻¹. (C) Propene produced versus incident laser power: propene GC/MS peak areas after irradiation of mixtures containing 212.5 Torr of cyclopropane and 50 Torr of nitrogen oxides for 30 s using the P(18) line of the (00¹)–(02⁰) transition, 1048.7 cm⁻¹. (D) 2-Propenal produced versus incident laser power: 2-propenal GC/MS peak areas after irradiation of mixtures containing 212.5 Torr of cyclopropane and 50 Torr of nitrogen oxides for 30 s using the P(18) line of the (00¹)–(02⁰) transition, 1048.7 cm⁻¹.

to 60 W cm⁻², allowed the assessment of the effect of varying laser powers on the quantities of products formed. These experiments were limited by the small quantity of cyclobutane available. The cyclobutane areas after irradiation were constant over the power range used, but the decrease in the area of the nitrogen oxides peak (Fig. 19) shows that more of the nitrogen oxides were consumed at higher laser powers. Both the infrared and GC/MS analyses (Fig. 20) showed that nitrocyclobutane production rose slightly with increase in irradiation power. The production of 1-nitropropane and the mixed gases displayed no clear dependence on the laser power, as judged by GC/MS peak areas. The amount of NO increased with increasing laser power. Fig. 21(A) and (B) show the production trends for 2-butene and ethene. The data acquired for the power series of experiments are limited but the overall trends for the production of the compounds are

believable in the light of the similar production curves seen in the cyclopropane experiments and in the cyclobutane pressure experiments described above. Increasing the laser power has the same effect on the product formation as increasing the cyclobutane pressure; this is not expected, since the cyclobutane is the energy-absorbing species in the reaction mixtures.

The effect of varying the irradiation time (30–120 s) on the trends of product formation was investigated using a series of experiments in which the cyclobutane and nitrogen oxide pressures were fixed at 179 and 40 Torr, respectively, and the laser power was set to 50 W cm⁻². The cyclobutane areas after irradiation were constant over the time range. Fig. 22(A) shows the depletion curve for the nitrogen oxides. The quantity of nitrocyclobutane formed increased only slightly, if at all, as the irradiation time increased over the 30–120 s

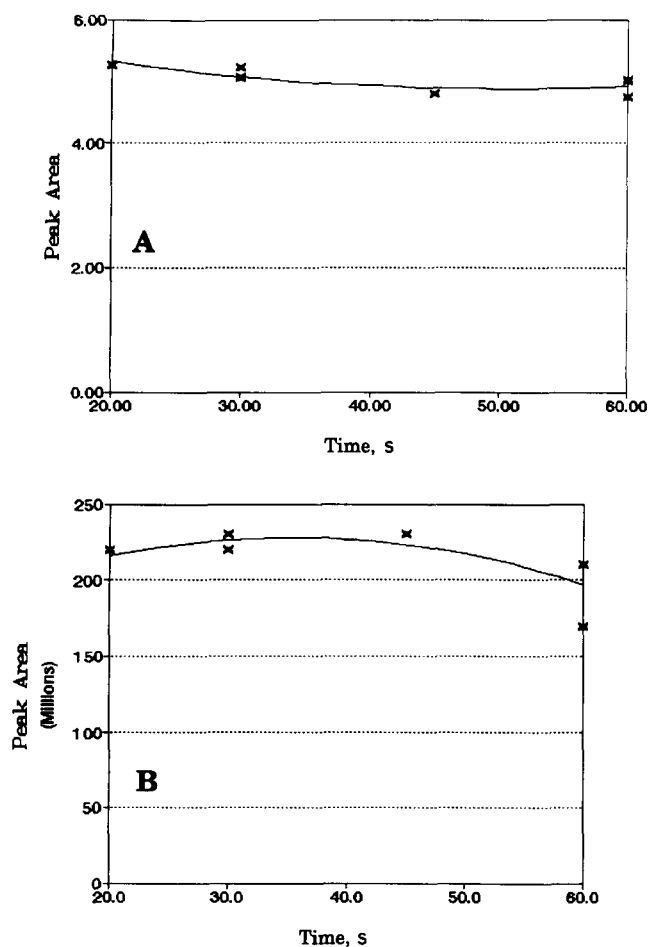


Fig. 12. Cyclopropane (209 Torr) remaining versus irradiation time after irradiation of mixtures containing 40 Torr of nitrogen oxides at 25 W cm^{-2} using the P(18) line of the $(00^{\circ}1)-(02^{\circ}0)$ transition, 1048.7 cm^{-1} : (A) cyclopropane infrared peak areas; (B) cyclopropane GC/MS peak areas.

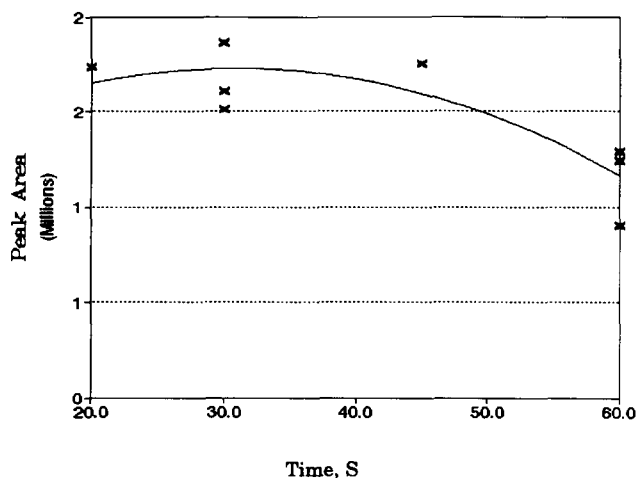


Fig. 13. Propene production versus irradiation time: propene GC/MS peak areas after irradiation of mixtures containing 209 Torr of cyclopropane and 40 Torr of nitrogen oxides at 25 W cm^{-2} using the P(18) line of the $(00^{\circ}1)-(02^{\circ}0)$ transition, 1048.7 cm^{-1} .

range. Formic acid reached a maximum between 60 and 90 s while the CO_2 formation continued to rise over the time range. Longer irradiation times favored the production of ethene

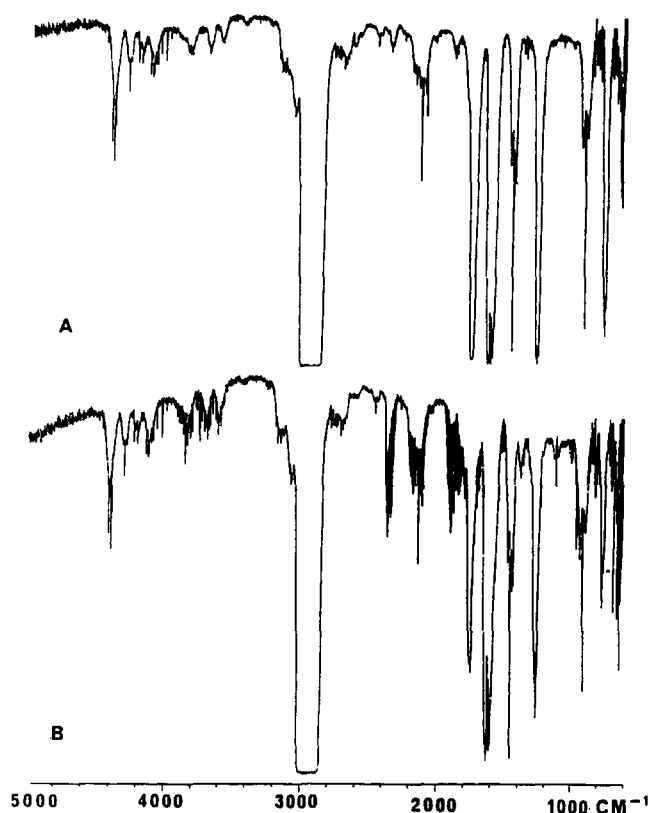


Fig. 14. Gas-phase mid-infrared spectra of cyclobutane- NO_2 mixture before excitation and products resulting from the CO_2 laser excitation of the mixture: (A) spectrum of cyclobutane (199.9 Torr) and NO_2 (40.0 Torr); (B) spectrum of products formed from the CO_2 laser excitation of the mixture in (A) under the conditions P(42) of $(00^{\circ}1)-(10^{\circ}0)$, 922.9 cm^{-1} , 60 W cm^{-2} , 60 s.

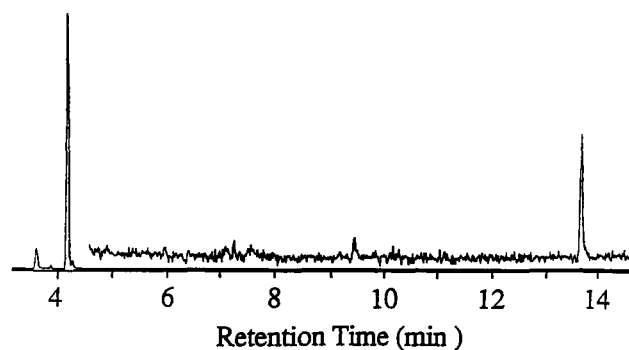


Fig. 15. Gas chromatogram from the analysis of the product mixture from the CO_2 laser excitation of 179.3 Torr of cyclobutane and 40.0 Torr of NO_2 for 60 s at 50 W cm^{-2} laser power on the P(42) line of the $(00^{\circ}1)-(10^{\circ}0)$ transition, 922.9 cm^{-1} .

Table 2
Infrared frequency regions for integrals of reactants and products in the cyclobutane and nitrogen oxides systems

Frequency interval (cm^{-1})	Identity
1500.9–1400.1	Cyclobutane
1296.0–1228.0	N_2O_4
952.7–945.9	Ethene
778.2–720.3	$\text{N}_2\text{O}_4 + \text{NO}_2$

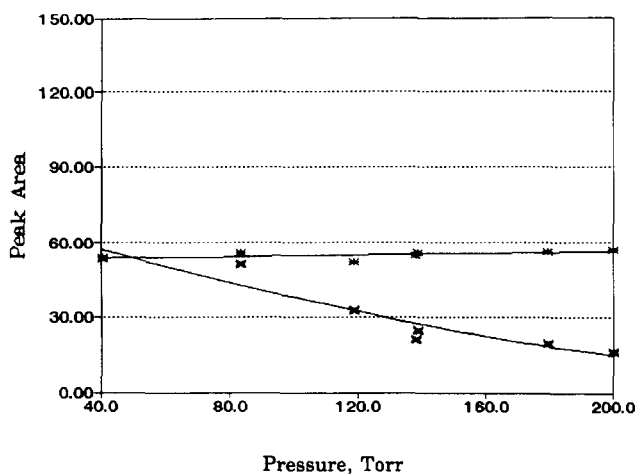


Fig. 16. Nitrogen oxides (40 Torr) depletion versus cyclobutane pressure: $\text{N}_2\text{O}_4 + \text{NO}_2$ infrared peak areas before and after irradiation for 60 s at 60 W cm^{-2} using the P(42) line of the $(00^{\circ}1)-(10^{\circ}0)$ transition, 922.9 cm^{-1} .

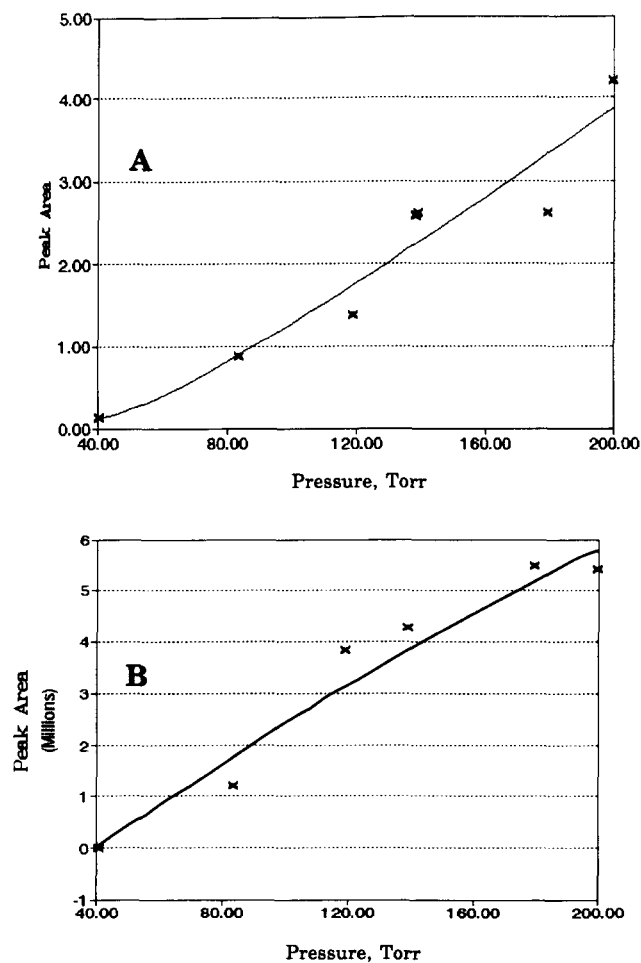


Fig. 17. Nitrocyclobutane formation versus cyclobutane pressure after irradiation of mixtures containing 40 Torr of nitrogen oxides for 60 s at 60 W cm^{-2} using the P(42) line of the $(00^{\circ}1)-(10^{\circ}0)$ transition, 922.9 cm^{-1} : (A) nitrocyclobutane infrared peak areas; (B) nitrocyclobutane GC/MS peak areas.

[Fig. 22(B)], perhaps at the expense of 2-butene [Fig. 22(C)]. The NO formation increased smoothly as the irradiation time increased. The mixed gas and 1-nitropropane GC peak areas showed little, if any, dependence on irradiation time.

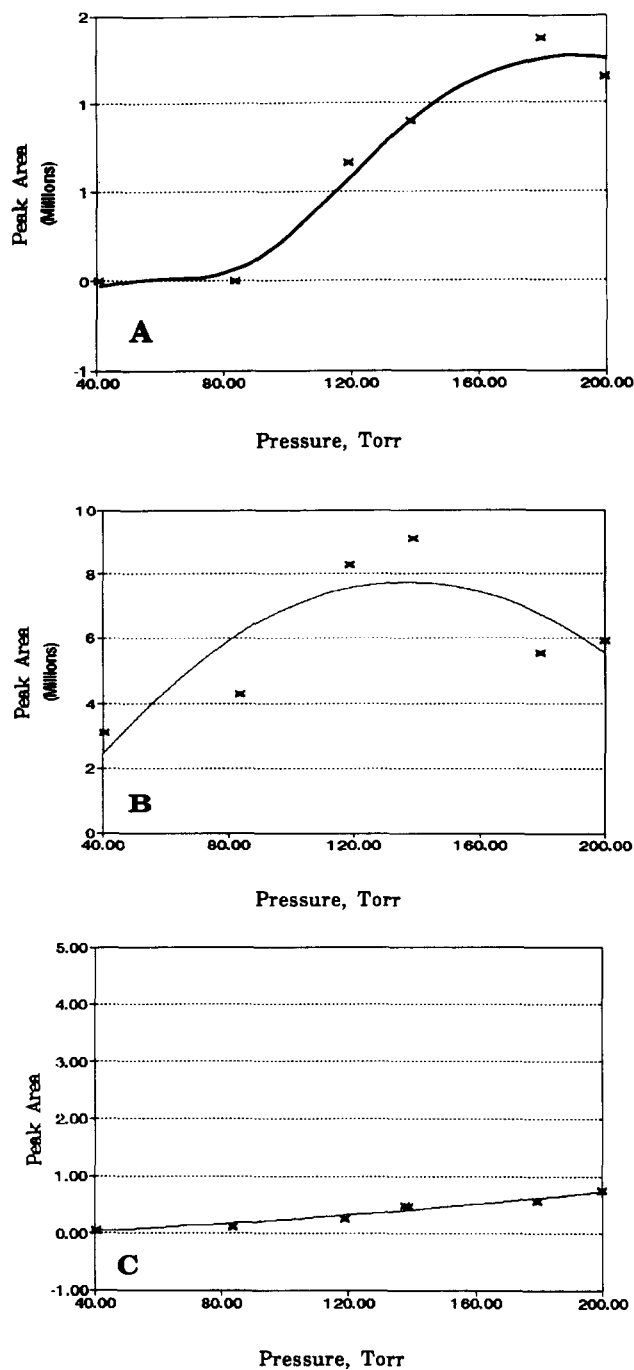


Fig. 18. (A) 1-Nitropropane production versus cyclobutane pressure: 1-nitropropane GC/MS peak areas after irradiation of mixtures containing 40 Torr of nitrogen oxides for 60 s at 60 W cm^{-2} using the P(42) line of the $(00^{\circ}1)-(10^{\circ}0)$ transition, 922.9 cm^{-1} . (B) 2-Butene production versus cyclobutane pressure: 2-butene GC/MS peak areas after irradiation of mixtures containing 40 Torr of nitrogen oxides for 60 s at 60 W cm^{-2} using the P(42) line of the $(00^{\circ}1)-(10^{\circ}0)$ transition, 922.9 cm^{-1} . (C) Ethene production versus cyclobutane pressure: ethene infrared peak areas after irradiation of mixtures containing 40 Torr of nitrogen oxides for 60 s at 60 W cm^{-2} using the P(42) line of the $(00^{\circ}1)-(10^{\circ}0)$ transition, 922.9 cm^{-1} .

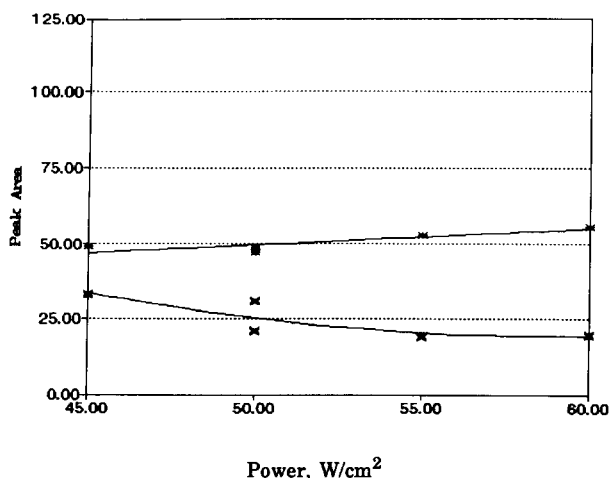


Fig. 19. Nitrogen oxides (40 Torr) depletion versus incident laser power: $\text{N}_2\text{O}_4 + \text{NO}_2$ infrared peak areas before and after irradiation of mixtures containing 179 Torr of cyclobutane for 60 s using the P(42) line of the $(00^01)-(10^00)$ transition, 922.9 cm^{-1} .

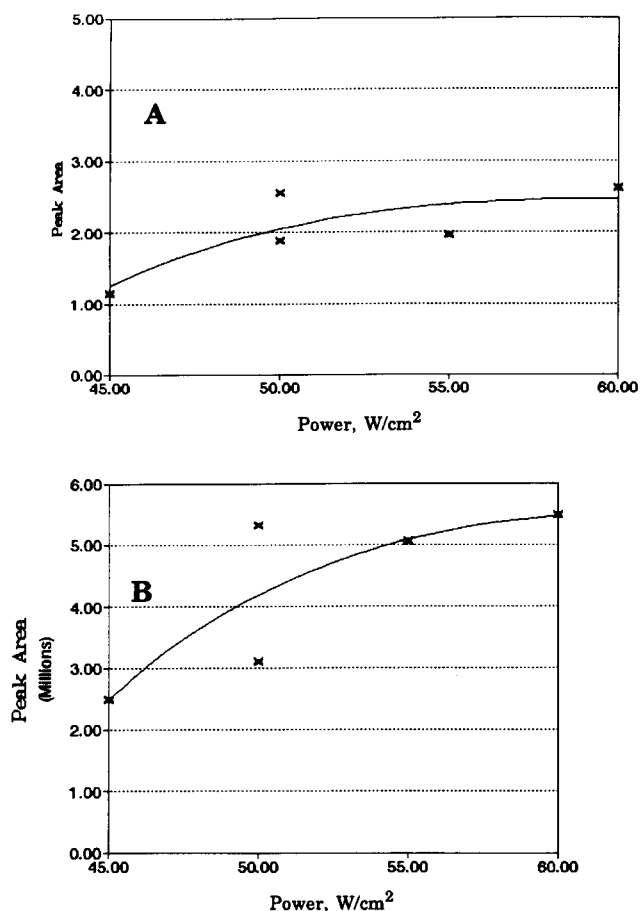


Fig. 20. Nitrocyclobutane formation versus incident laser power after irradiation of mixtures containing 179 Torr of cyclobutane and 40 Torr of nitrogen oxides for 60 s using the P(42) line of the $(00^01)-(10^00)$ transition, 922.9 cm^{-1} : (A) nitrocyclobutane infrared peak areas; (B) nitrocyclobutane GC/MS peak areas.

3.3. Cyclopentane

Cyclopentane has a single weak infrared absorption band which is centered at 897 cm^{-1} , lying on the edge of the usable

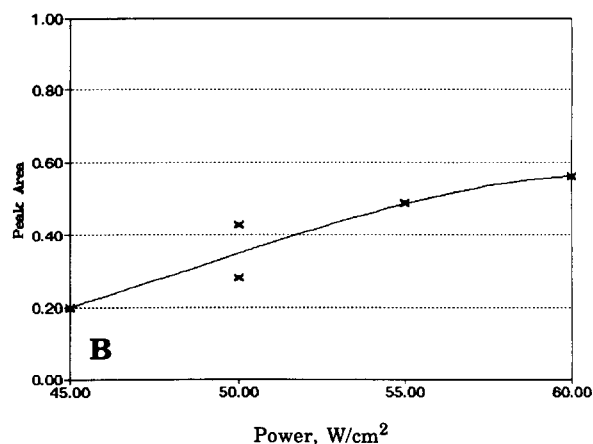
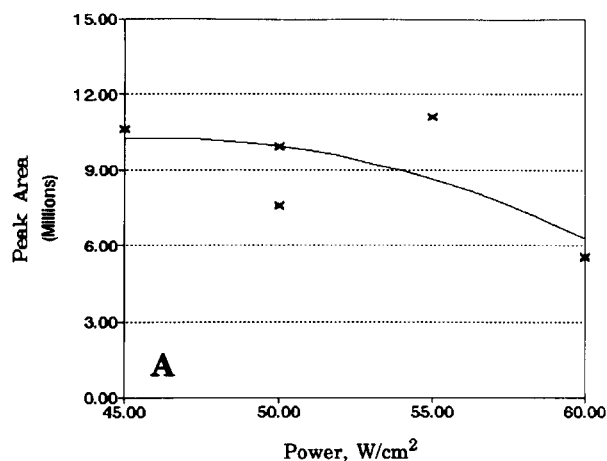


Fig. 21. (A) 2-Butene production versus incident laser power: 2-butene GC/MS peak areas after irradiation of mixtures containing 179 Torr of cyclobutane and 40 Torr of nitrogen oxides for 60 s using the P(42) line of the $(00^01)-(10^00)$ transition, 922.9 cm^{-1} . (B) Ethene production versus incident laser power: ethene infrared peak areas after irradiation of mixtures containing 179 Torr of cyclobutane and 40 Torr of nitrogen oxides for 60 s using the P(42) line of the $(00^01)-(10^00)$ transition, 922.9 cm^{-1} .

range of the carbon dioxide laser. Direct irradiation of the cyclopentane was possible only on the R-branch shoulder of the absorption band. To increase the efficiency of the irradiation of cyclopentane, an infrared sensitizer, sulfur hexafluoride, was sometimes introduced into the cyclopentane nitrogen oxide system. Sulfur hexafluoride has a strong infrared absorption (maximum at 945 cm^{-1}), permitting irradiation at 946.0 cm^{-1} , which corresponds to the frequency of the P(18) line of the $(00^01)-(10^00)$ band, an intense output line of the CO_2 laser. When the mixtures were irradiated using the P(18) line, the energy absorbed by the system depended on the pressure of SF_6 rather than on that of cyclopentane. Typical infrared spectra and gas chromatograms are shown in Figs. 23 and 24. Mixtures of cyclopentane (180 Torr) and nitrogen oxides (25 Torr) were irradiated at 50 W cm^{-2} with SF_6 present in small amounts (0.2 and 0.5 Torr). Some of the frequency intervals over which integrals were acquired for the reactants, products and sensitizer are listed in Table 3. As expected, the area of the sensitizer SF_6 remained flat over the irradiation time range 0–60 s. Sensitizers do not

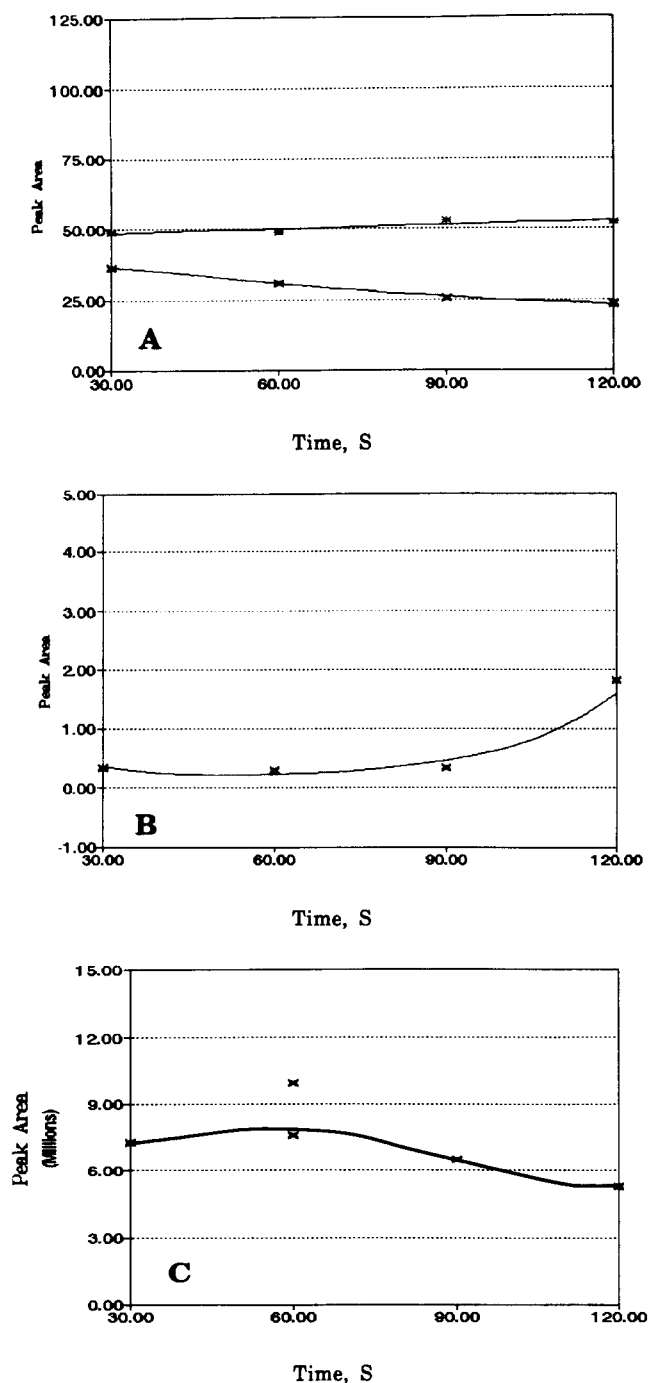


Fig. 22. (A) Nitrogen oxides (40 Torr) versus irradiation time: $\text{N}_2\text{O}_4 + \text{NO}_2$ infrared peak areas before and after irradiation of mixtures containing 179 Torr of cyclobutane at 50 W cm^{-2} using the P(42) line of the $(00^01)-(10^00)$ transition, 922.9 cm^{-1} . (B) Ethene production versus irradiation time: ethene infrared peak areas after irradiation of mixtures containing 179 Torr of cyclobutane and 40 Torr of nitrogen oxides at 50 W cm^{-2} using the P(42) line of the $(00^01)-(10^00)$ transition, 922.9 cm^{-1} . (C) 2-Butene production versus irradiation time: 2-butene GC/MS peak areas after irradiation of mixtures containing 179 Torr of cyclobutane and 40 Torr of nitrogen oxides at 50 W cm^{-2} using the P(42) line of the $(00^01)-(10^00)$ transition, 922.9 cm^{-1} .

change chemically in the course of the reaction. The cyclopentane areas appeared to remain constant over the entire time range (Fig. 25); however, the quantity of nitrogen

oxides after irradiation (Fig. 26) diminished rapidly as the irradiation time increased, an effect that was especially dramatic in the reactions containing 0.5 Torr of SF_6 . GC/MS analysis using the gas sampling loop showed that irradiation of mixtures containing SF_6 at these two pressures produced significant quantities of nitrocyclopropane, in addition to 1-nitrobutane and 1-nitropropane. The quantity of nitrocyclo-

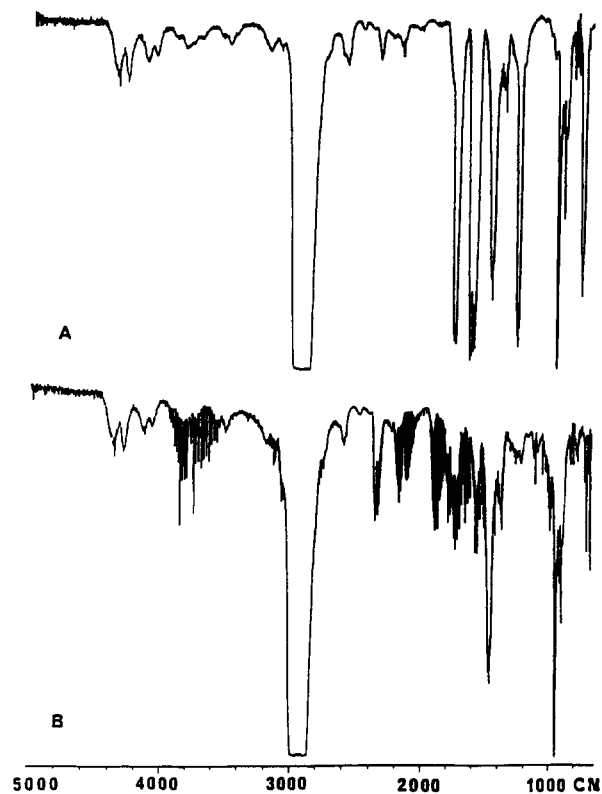


Fig. 23. Gas-phase mid-infrared spectra of cyclopentane- NO_2 mixture before excitation and products resulting from the CO_2 laser excitation of the mixture: (A) spectrum of cyclopentane (168 Torr), NO_2 (32 Torr) and SF_6 (2.0 Torr); (B) spectrum of products formed under the CO_2 laser excitation of the mixture in (A) under the conditions P(46) of $(00^01)-(10^00)$, 918.7 cm^{-1} , 45 W cm^{-2} , 60 s.

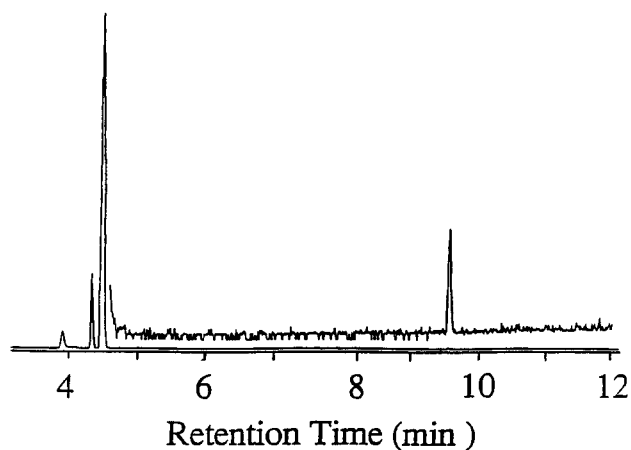


Fig. 24. Gas chromatogram from the analysis of the product mixture from the CO_2 laser excitation of 168.9 Torr of cyclopentane, 30.9 Torr of NO_2 and 0.4 Torr of SF_6 for 60 s at 45 W cm^{-2} laser power on the P(46) line of the $(00^01)-(10^00)$ transition, 918.7 cm^{-1} .

Table 3

Infrared frequency regions for integrals of reactants and products in the cyclopentane and nitrogen oxides systems

Frequency interval (cm^{-1})	Identity
1286.8–1230.9	N_2O_4
955.1–934.9	SF_6
920.4–871.2	Cyclopentane
779.1–720.8	$\text{N}_2\text{O}_4 + \text{NO}_2$

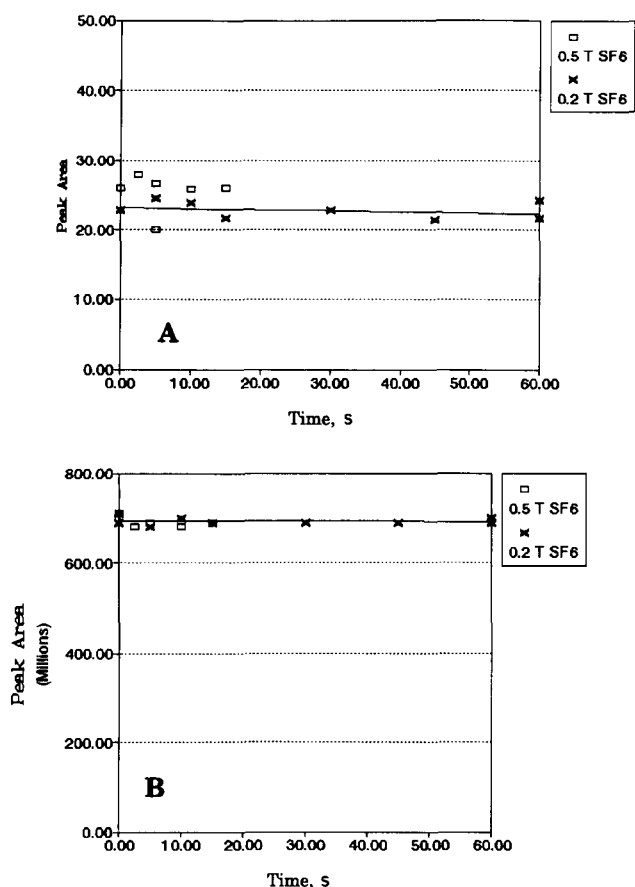


Fig. 25. Cyclopentane remaining versus irradiation time at two SF_6 pressures (0.2 and 0.5 Torr) after irradiation of cyclopentane (180 Torr) and nitrogen oxides (25 Torr) at 50 W cm^{-2} using the P(18) line of the $(00^01)-(10^00)$ transition, 946.0 cm^{-1} : (A) cyclopentane infrared peak areas; (B) cyclopentane GC/MS peak areas.

pentane in the vapor phase reached a maximum earlier in the reactions containing 0.5 Torr of SF_6 (Fig. 27), with the quantity leveling off after a reaction time of about 15 s. When the SF_6 pressure was 0.2 Torr, the maximum nitrocyclopentane was reached at 45 s; however, the same maximum amount of product was detected in both reactions. Figs. 27 and 28 show that 1-nitrobutane and 1-nitropropane are formed earlier and in greater amounts when 0.5 Torr of SF_6 is present. The products reached a maximum at 10–15 s in the 0.5 Torr experiments and at 45 s in the 0.2 Torr experiments. The gaseous products CO_2 , CO and NO , were formed in much the same manner. The production of nitroalkanes was not

monitored by infrared measurements owing to overlapping absorbances in the regions of interest. Formic acid production was monitored but the time dependence of its production

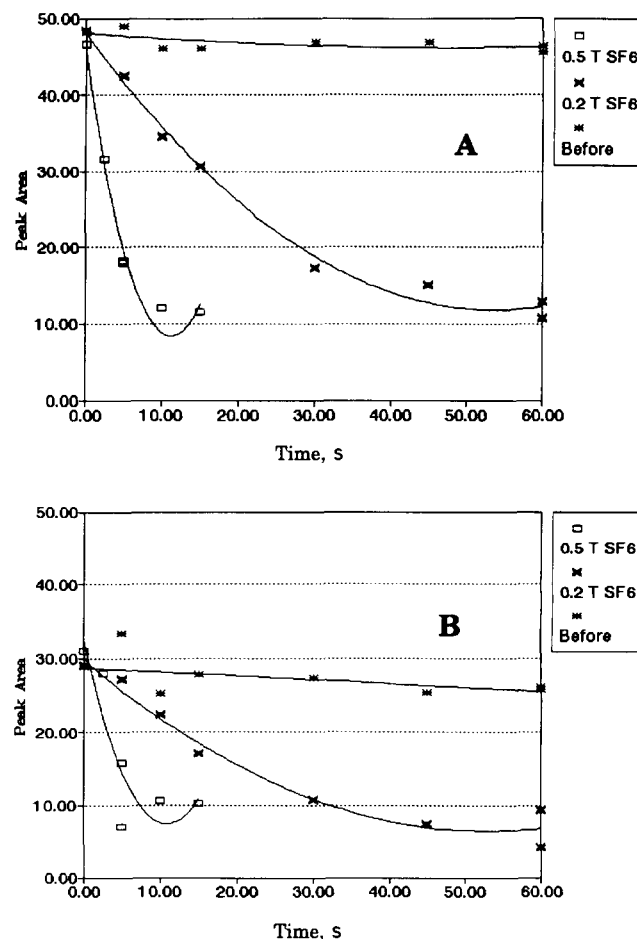


Fig. 26. Nitrogen oxides depletion versus irradiation time at two SF_6 pressures (0.2 and 0.5 Torr) before and after irradiation of cyclopentane (180 Torr) and nitrogen oxides (25 Torr) at 50 W cm^{-2} using the P(18) line of the $(00^01)-(10^00)$ transition, 946.0 cm^{-1} : (A) N_2O_4 infrared peak areas; (B) $\text{N}_2\text{O}_4 + \text{NO}_2$ infrared peak areas.

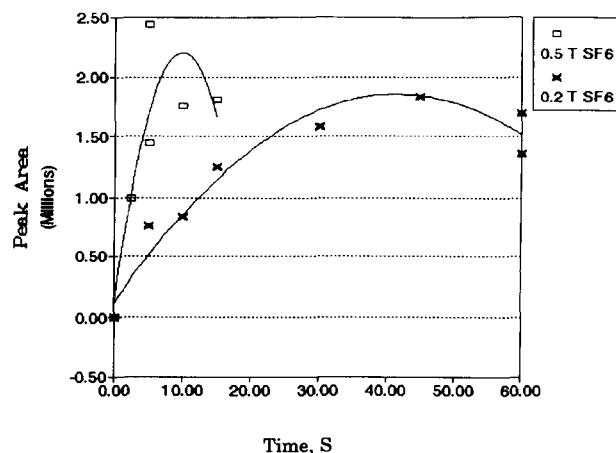


Fig. 27. Nitrocyclopentane formation versus irradiation time at two SF_6 pressures (0.2 and 0.5 Torr): nitrocyclopentane GC/MS peak areas after irradiation of cyclopentane (180 Torr) and nitrogen oxides (25 Torr) at 50 W cm^{-2} using the P(18) line of the $(00^01)-(10^00)$ transition, 946.0 cm^{-1} .

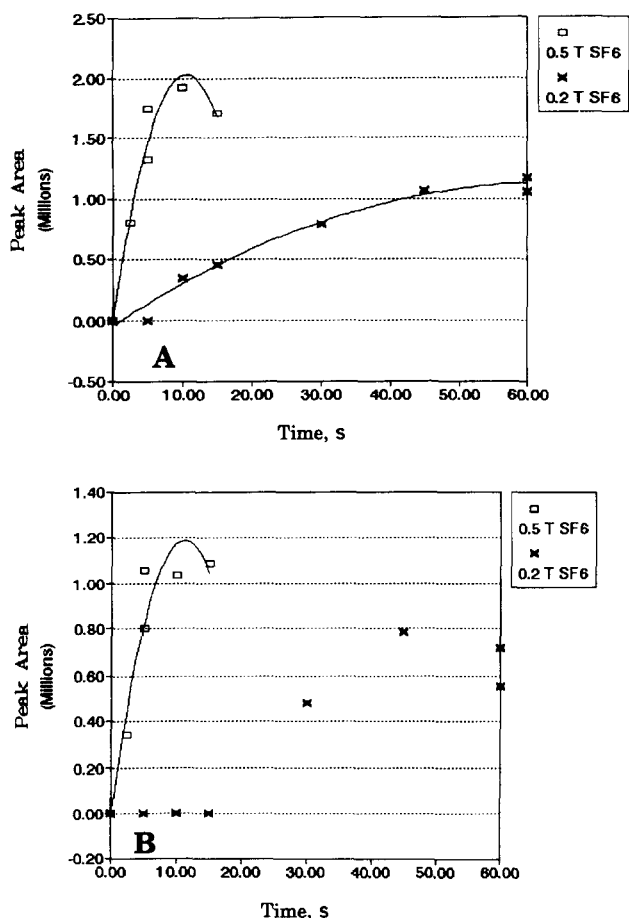


Fig. 28. (A) 1-Nitrobutane formation versus irradiation time at two SF₆ pressures (0.2 and 0.5 Torr): 1-nitrobutane GC/MS peak areas after irradiation of cyclopentane (180 Torr) and nitrogen oxides (25 Torr) at 50 W cm⁻² using the P(18) line of the (00⁰1)–(10⁰) transition, 946.0 cm⁻¹. (B) 1-Nitropropane formation versus irradiation time at two SF₆ pressures (0.2 and 0.5 Torr): 1-nitropropane GC/MS peak areas after irradiation of cyclopentane (180 Torr) and nitrogen oxides (25 Torr) at 50 W cm⁻² using the P(18) line of the (00⁰1)–(10⁰) transition, 946.0 cm⁻¹.

could not be determined. As indicated by GC/MS analysis [4], pressures of SF₆ greater than about 1 Torr resulted in extensive fragmentation of cyclopentane and little nitrocyclopentane, making irradiation using the 946.0 cm⁻¹ line futile. The high absorptivity of the SF₆ band near the 946.0 cm⁻¹ laser line coupled with the difficulty in controlling the laser power below about 25 W cm⁻² created a reaction system which was too sensitive to small changes in the SF₆ pressures. Therefore, conditions were sought which would allow the use of higher SF₆ pressures.

The SF₆ absorption band is narrow but extremely intense, so that significant laser power is absorbed by SF₆ even at frequencies offset from its maximum absorbance by more than 25 cm⁻¹. The P(46) line of the (00⁰1)–(10⁰) transition at 918.7 cm⁻¹ provides access to the overlapping absorptions of SF₆ and cyclopentane, both of which absorb weakly [3] at 918.7 cm⁻¹. When irradiated using the P(46) laser line, cyclopentane absorbed enough energy so that nitration occurred even in the absence of SF₆. After mixtures of cyclo-

pentane (180 Torr) and NO₂ (20 Torr) were irradiated at 45 W cm⁻² for times ranging from 0 to 120 s, the amount of cyclopentane remaining had not decreased significantly. The amount of nitrocyclopentane, the only nitroalkane detected in these mixtures, increased in the vapor phase up to an irradiation time of about 60 s, beyond which its production leveled off (Fig. 29). Mixed gas production followed the same pattern. This result indicates that increasing the irradiation time does favor fragmentation processes.

Mixtures containing cyclopentane (180 Torr), nitrogen oxides (20 Torr) and varying amounts of SF₆ (0–3.0 Torr) were irradiated for 60 s at 45 W cm⁻² using the P(46) transition. The area of the GC/MS peak from cyclopentane indicated that more of it was consumed as the pressure of the sensitizer increased [Fig. 30(A)]. Using the P(46) laser line with 1.0–2.0 Torr of SF₆ facilitated the production of nitrocyclopentane [Fig. 30(B)], but as more energy was absorbed by the system (higher SF₆ pressures) the quantity of the nitrocyclopentane produced in the gas phase decreased. Moderate pressures of SF₆ also favored the production of 1-nitrobutane and 1-nitropropane: GC/MS analyses indicated that there was a narrow range of SF₆ pressures (between 1 and 2 Torr) over which the straight-chain nitroalkanes could be detected. In contrast, as the amount of SF₆ in the system increased, mixed gas production rose sharply owing to fragmentations yielding small molecules, a process which is favored in the higher energy reactions.

Irradiation of the reaction mixtures containing SF₆ frequently produced visible quantities of a liquid on the potassium chloride windows. Since the vapor pressure of nitrocyclopentane is low (about 1 Torr), we were suspicious that some conditions contributed to the formation of nitrocyclopentane in both the vapor and the condensed phases. For this reason, the cell wash procedure described in the

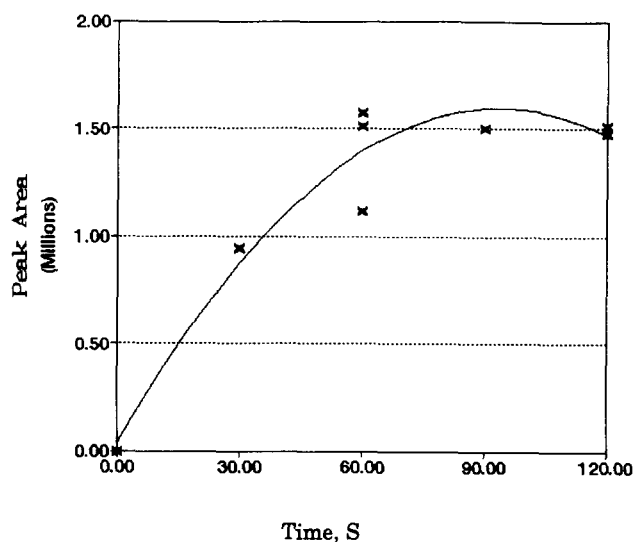


Fig. 29. Nitrocyclopentane formation versus irradiation time: nitrocyclopentane GC/MS peak areas after irradiation of cyclopentane (180 Torr) and nitrogen oxides (20 Torr) at 45 W cm⁻² using the P(46) line of the (00⁰1)–(10⁰) transition, 918.7 cm⁻¹.

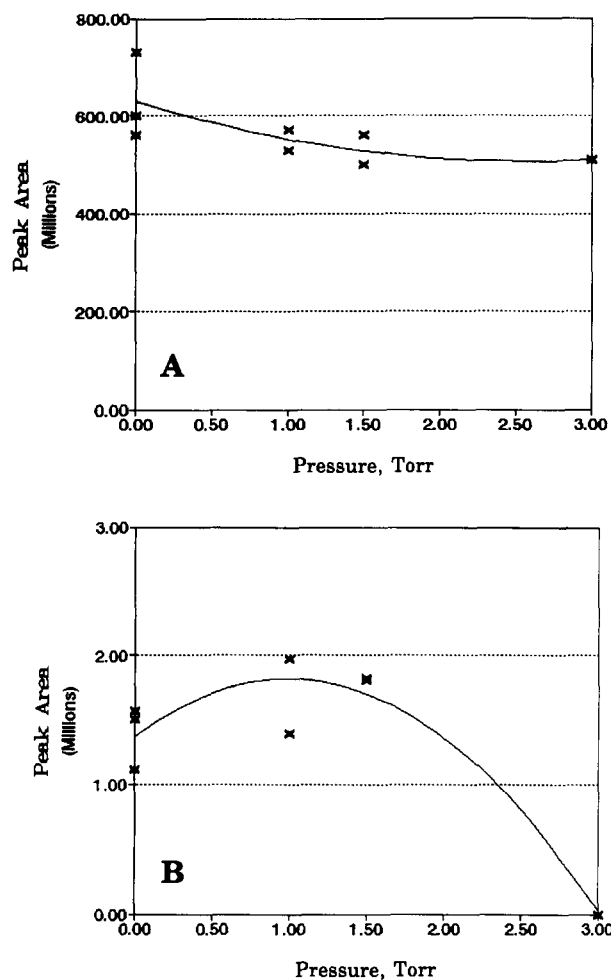


Fig. 30. (A) Cyclopentane remaining versus SF₆ pressure: cyclopentane GC/MS peak areas after irradiation of cyclopentane (180 Torr) and nitrogen oxides (20 Torr) at 45 W cm⁻² using the P(46) line of the (00¹)–(10⁰) transition, 918.7 cm⁻¹. (B) Nitrocyclopentane production versus SF₆ pressure: nitrocyclopentane GC/MS peak areas after irradiation of cyclopentane (180 Torr) and nitrogen oxides (20 Torr) at 45 W cm⁻² using the P(46) line of the (00¹)–(10⁰) transition, 918.7 cm⁻¹.

experimental section was used to monitor liquid-phase products in the experiments that follow.

The effect of irradiation time with small amounts of SF₆ present was investigated using the P(46) transition at 45 W cm⁻² to excite mixtures of cyclopentane (170 Torr), nitrogen oxides (30 Torr) and SF₆ (0.5 Torr). Irradiation times ranging from 60 to 240 s resulted in no detectable drop in the cyclopentane peak areas as measured by both GC/MS and infrared analysis. However, the nitrogen oxide reactants were significantly depleted over this time range, as Fig. 31 shows. Increasing the irradiation time beyond 60 s did not facilitate nitrocyclopentane production. Fig. 32(A) presents the results of the GC/MS analyses for nitrocyclopentane using the gas sampling loop. Following gas sampling, 2.0 ml aliquots of absolute ethanol were used as a cell rinse. Samples (0.5 ml of cell wash) were injected into the GC/MS system, the replicate peak areas averaged and the results plotted. Nitrocyclopentane was the only product detected in the cell wash.

As Fig. 32(B) indicates, irradiation times longer than 60 s did not result in more liquid nitrocyclopentane. The GC/MS areas in Fig. 32(B) can be compared with those from the gas sampling experiment if we take into account the relative amount of samples injected by each method. In the cell-wash experiment a 0.5 ml injection represented 0.025% of the total sample; in the gas sampling experiment a 0.250 ml aliquot represented 0.25% of the total sample. To compare the results of the two experiments, the peak areas in the cell-wash experiment must therefore be multiplied by 10. Fig. 32(A) and (B) show that about 10 times as much nitrocyclopentane exists in the liquid phase as in the gas phase after 60 s of irradiation, and that irradiation for longer times does not alter the amounts of products formed in either phase. The mass of nitrocyclopentane formed was estimated by mimicking the manner in which the cell washes were conducted. The peak area from the 60 s irradiation corresponded to about 1 mg of nitrocyclopentane (5% yield, based on moles of nitrogen oxides present initially). Although no other nitroalkanes were

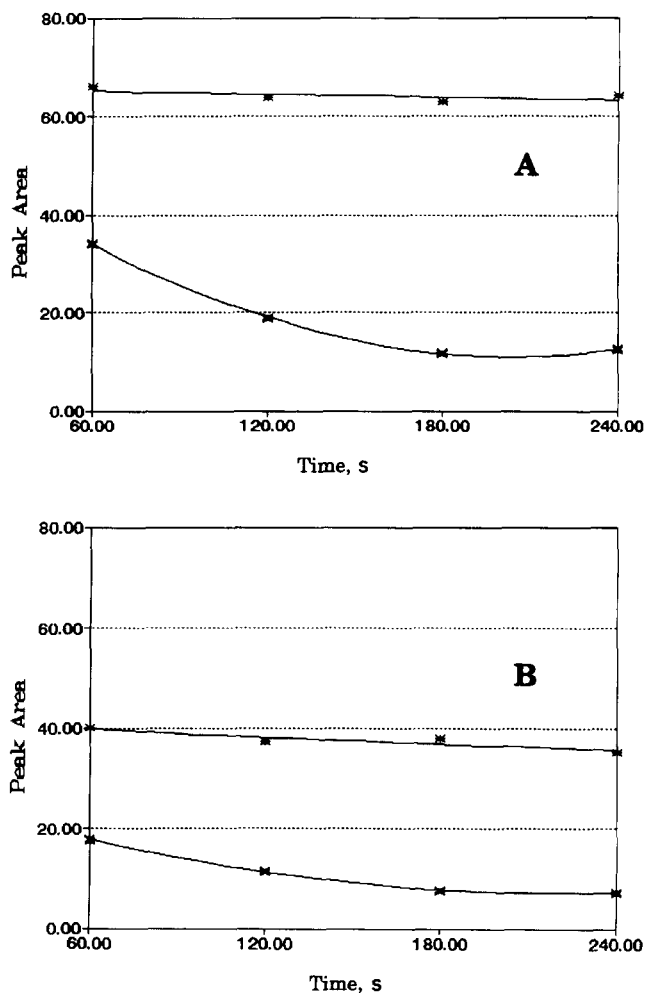


Fig. 31. Nitrogen oxides (30 Torr) depletion versus irradiation time before and after irradiation of mixtures containing 170 Torr of cyclopentane and 0.5 Torr of SF₆ at 45 W cm⁻² using the P(46) line of the (00¹)–(10⁰) transition, 918.7 cm⁻¹: (A) N₂O₄ infrared peak areas; (B) N₂O₄ + NO₂ infrared peak areas.

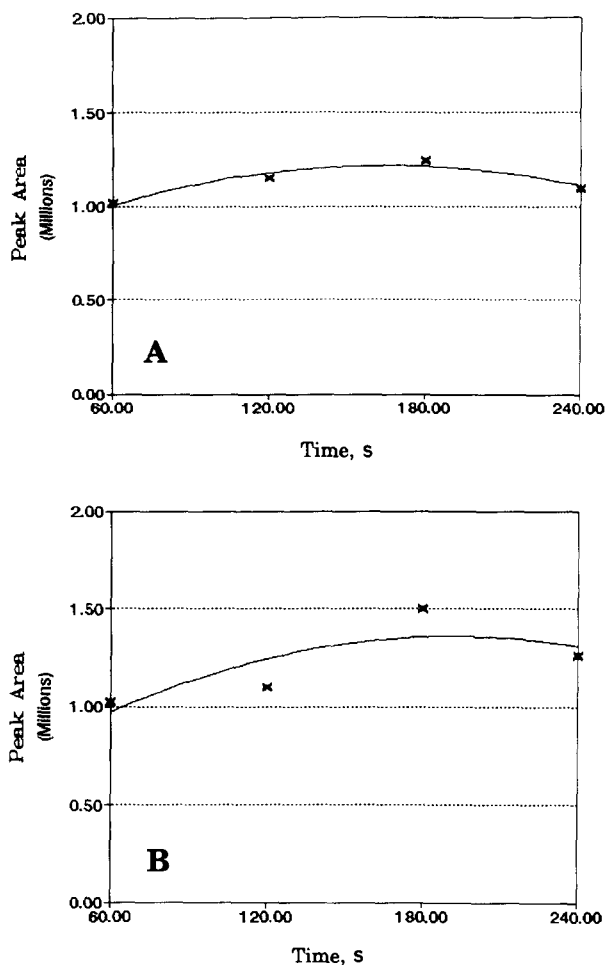


Fig. 32. (A) Nitrocyclopentane vapor analysis versus irradiation time: nitrocyclopentane GC/MS peak areas after irradiation of mixtures containing 170 Torr of cyclopentane, 30 Torr of nitrogen oxides and 0.5 Torr of SF₆ at 45 W cm⁻² using the P(46) line of the (00¹)–(10⁰) transition, 918.7 cm⁻¹. (B) Nitrocyclopentane liquid analysis versus irradiation time: nitrocyclopentane cell wash GC/MS peak areas after irradiation of mixtures containing 170 Torr of cyclopentane, 30 Torr of nitrogen oxides and 0.5 Torr of SF₆ at 45 W cm⁻² using the P(46) line of the (00¹)–(10⁰) transition, 918.7 cm⁻¹.

detected, increasing irradiation times did encourage formic acid, CO₂ and NO production. The CO production does not depend on the irradiation time. The area of the mixed gas peak displayed, if anything, a slight decrease over irradiation times ranging from 60 to 240 s. This result supports previous observations: increasing the irradiation times does not favor fragmentation processes as strongly as does increasing the pressure of the sensitizer SF₆, which encourages the formation of the mixed gases through a strong energy-absorbing effect.

The results of previous experiments in which SF₆ pressure was varied indicated that nitrocyclopentane production decreased as the SF₆ pressure exceeded 1.5 Torr, perhaps as a result of depletion of nitrogen oxides (initially 20 Torr) from the reaction mixtures. Using infrared and GC/MS analyses, the profiles of products resulting from a series of reaction mixtures in which the SF₆ pressure was carefully

controlled (0–2.5 Torr), the cyclopentane pressure was 170 Torr and the nitrogen oxides pressure was increased to 30 Torr were examined. Irradiation was carried out for 60 s at 45 W cm⁻² using the P(46) line. The areas of the SF₆ peaks increased linearly with increasing SF₆ pressure, and were the same before and after irradiation, showing the sensitizer's stability. Cyclopentane areas in the product mixtures did not appear to decrease as the SF₆ pressure rose according to the GC/MS analyses. Our efforts to follow any decrease in cyclopentane using infrared integrals were hindered at higher SF₆ pressures by the formation of ethene, many of whose infrared transitions overlap the spectral region which was monitored for cyclopentane, 920.4–871.2 cm⁻¹. The unreacted nitrogen oxides showed a marked dependence on SF₆ pressure, having reacted almost completely at 2.0 Torr of SF₆ (Fig. 33).

Nitrocyclopentane remained constant in the gas phase from 0 to 2.0 Torr of SF₆, and then decreased at 2.5 Torr [Fig. 34(A)]. The cell wash results help to explain the nitrocyclopentane production. Sufficient nitrocyclopentane had formed at 0 Torr of SF₆ for it to be detected in the condensed phase

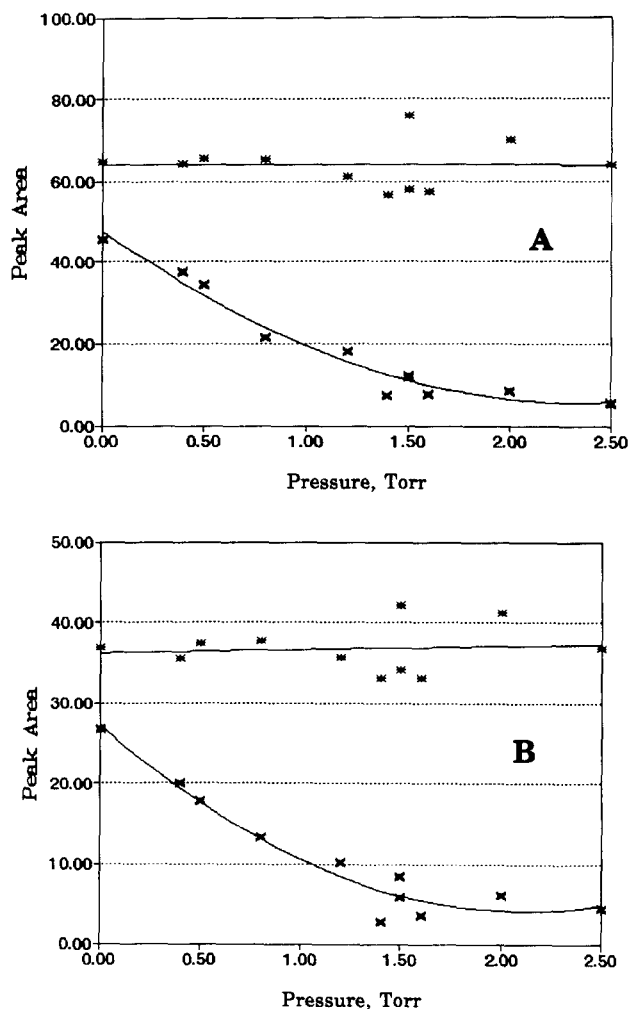


Fig. 33. Nitrogen oxides (30 Torr) depletion versus SF₆ pressure before and after irradiation of mixtures containing 170 Torr of cyclopentane for 60 s at 45 W cm⁻² using the P(46) line of the (00¹)–(10⁰) transition, 918.7 cm⁻¹: (A) N₂O₄ infrared peak areas; (B) N₂O₄ + NO₂ infrared peak areas.

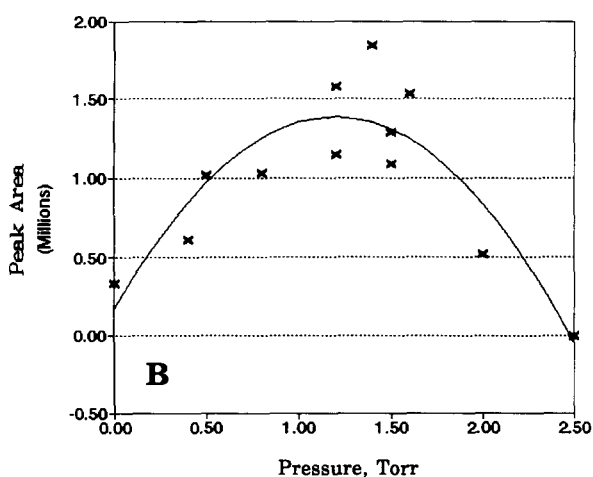
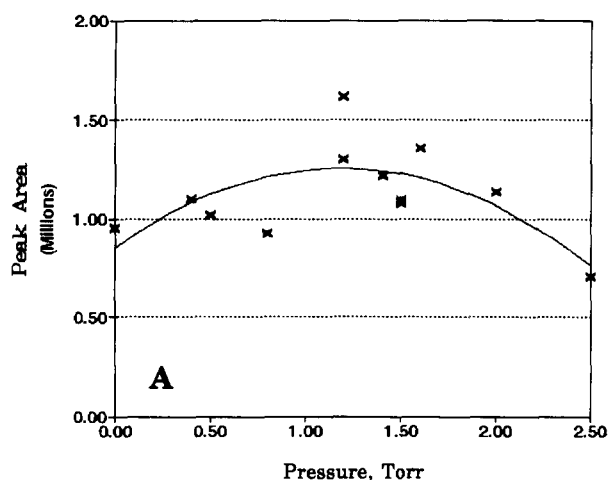


Fig. 34. (A) Nitrocyclopentane vapor analysis versus SF_6 pressure: nitrocyclopentane GC/MS peak areas after irradiation of mixtures containing 170 Torr of cyclopentane and 30 Torr of nitrogen oxides for 60 s at 45 W cm^{-2} using the P(46) line of the $(00^{\circ}1)-(10^{\circ}0)$ transition, 918.7 cm^{-1} . (B) Nitrocyclopentane liquid analysis versus SF_6 pressure: nitrocyclopentane cell wash GC/MS peak areas after irradiation of mixtures containing 170 Torr of cyclopentane and 30 Torr of nitrogen oxides for 60 s at 45 W cm^{-2} using the P(46) line of the $(00^{\circ}1)-(10^{\circ}0)$ transition, 918.7 cm^{-1} .

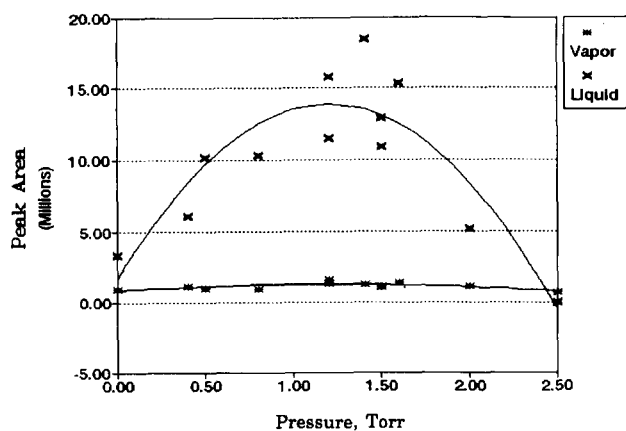


Fig. 35. Nitrocyclopentane vapor and cell wash (scaled $10\times$) areas versus SF_6 pressure after irradiation of cyclopentane (170 Torr) and nitrogen oxides (30 Torr) for 60 s at 45 W cm^{-2} using the P(46) line of the $(00^{\circ}1)-(10^{\circ}0)$ transition, 918.7 cm^{-1} .

[Fig. 34(B)], with the quantity in the liquid phase increasing up to about 1.5 Torr of SF_6 and the amount in the gas phase remaining constant and equal to the vapor pressure. From 1.5 to 2.5 Torr of SF_6 , the nitrocyclopentane production decreased until none was detected in the liquid phase and all that was produced was present in the vapor phase; at 2.5 Torr of SF_6 the reaction system was so energetic that products besides nitrocyclopentane were favored. Fig. 35, in which the condensed phase areas are scaled (factor $10\times$), displays a comparison of vapor-phase and condensed-phase nitrocyclopentane production. Linear nitroalkanes identified in this system were 1-nitrobutane and 1-nitropropane. Both products were undetected until the SF_6 pressure reached about 1 Torr, after which their production increased, peaking at about 1.5 Torr, and then decreased thereafter, until neither could be detected at 2.5 Torr of SF_6 [Fig. 36(A) and (B)]. Formic acid and CO_2 production increased up to SF_6 pressures of about 2 Torr, where the amounts leveled off, or perhaps decreased. In contrast, the amounts of CO and NO present in the product mixture continued to increase throughout the

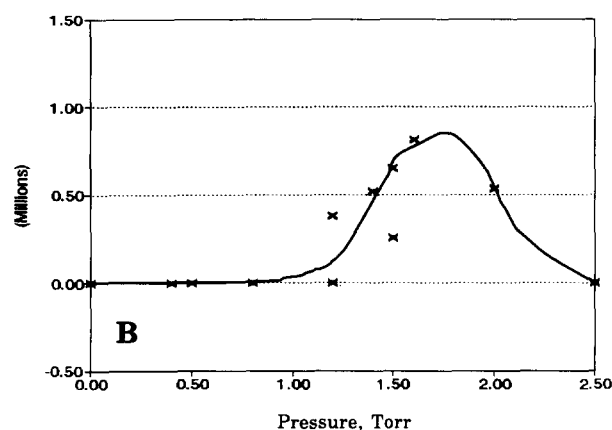
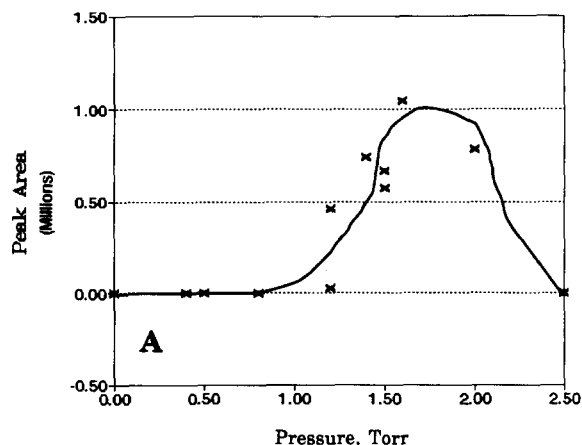


Fig. 36. (A) 1-Nitrobutane formation versus SF_6 pressure: 1-nitrobutane GC/MS peak areas after irradiation of mixtures containing 170 Torr of cyclopentane and 30 Torr of nitrogen oxides for 60 s at 45 W cm^{-2} using the P(46) line of the $(00^{\circ}1)-(10^{\circ}0)$ transition, 918.7 cm^{-1} . (B) 1-Nitropropane formation versus SF_6 pressure: 1-nitropropane GC/MS peak areas after irradiation of mixtures containing 170 Torr of cyclopentane and 30 Torr of nitrogen oxides for 60 s at 45 W cm^{-2} using the P(46) line of the $(00^{\circ}1)-(10^{\circ}0)$ transition, 918.7 cm^{-1} .

entire range of SF₆ pressures. The GC/MS mixed gas peak increased slightly up to about 1.5 Torr of SF₆, then inclined sharply when the sensitizer pressure exceeded 1.5 Torr, a reflection of the increased fragmentation that occurred as the rate of energy absorption by the system increased. Additional gaseous products resulting from the higher energy absorbed in the 2.0 and 2.5 Torr experiments were HCN, ethene, methane and tentatively, formaldehyde and NNO, as identified in the infrared spectra.

4. Conclusions

The CW CO₂ laser-induced nitration reactions between nitrogen oxides and cyclopropane, cyclobutane and cyclopentane were performed under a wide range of reaction conditions in order to evaluate the effectiveness and selectivity of the laser-driven processes. The utilization and correlation of both infrared areas and GC/MS areas indicates a high level of statistical accuracy for the discussed relationships. The impact of increased energy absorption was monitored on the products of greatest synthetic interest to us, the nitrocycloalkanes. Although the optimal conditions for nitration vary among the hydrocarbons, each has an optimal power window for producing nitrocycloalkanes without breaking down the precursors or products. For the cyclopropane experiments, the most favorable ratio of nitrocyclopropane to undesirable side products occurs when mixtures of cyclopropane (210 Torr) and nitrogen oxides (40 Torr) are irradiated at 25 W cm⁻² for 20–25 s using the P(18) laser line of the (00^o1)–(02^o0) transition. These conditions give no detectable amounts of side products that could pose separation problems, namely propene, nitromethane, propenal, acetonitrile and propenitrile, and an almost undetectable level of HCN. Using the P(42) line of the (00^o1)–(10^o0) transition, mixtures of cyclobutane (180 Torr) and nitrogen oxides (40 Torr), when irradiated at 50 W cm⁻² for 60 s, favor nitrocyclobutane production while minimizing 1-nitropropane. If 1-nitropropane can be tolerated in the product mixture, raising the power to 60 W cm⁻² while increasing the cyclobutane pressure to 200 Torr increases the amount of both nitroalkanes. In the cyclopentane nitration, the most favorable pressures are 170 Torr of cyclopentane, 30 Torr of nitrogen oxides and 1.0 Torr of SF₆ with irradiation at 45 W cm⁻² for 30 s using the P(46) line of the (00^o1)–(10^o0) transition of the CO₂ laser. These conditions yield nitrocyclopentane while eliminating detectable amounts of 1-nitrobutane and 1-nitropropane. Only at high SF₆ pressures (2.0 Torr) was trace HCN detected in the infrared spectra.

From the GC/MS and infrared analyses, the dependence of the quantity of reactants and products formed on either variations in the incident laser power or changes in pressures of the cyclic hydrocarbons, sensitizer and nitrogen oxides was found. The product yields, especially those of the nitrocycloalkanes, are highly sensitive to changes in the reaction systems, and therefore serve as a probe of the energy state of

the reaction. Energy absorption is increased by (a) irradiation for longer times while holding the pressures of the reactants and the incident power constant, (b) increasing the incident laser power, (c) increasing the pressure of the energy-absorbing hydrocarbon or (d) increasing the sensitizer pressure. Of these, increased irradiation time is unique in that it increases the total energy absorbed by the system without increasing the power absorbed (energy per unit time). Under a given set of pressures and incident power, the amount of nitrocycloalkane depends on irradiation time to the extent that the nitrogen oxides are still available in the reaction system. In fact, all the products, except ethene forming from cyclobutane, follow this pattern: the products reach their maximum yields by the time the pressures of the nitrogen oxides decrease and then level off, indicating that nitrogen oxides are required in the reaction paths of each of them.

Increased hydrocarbon pressure, incident laser power and sensitizer pressure all have the effect of increasing the rate of energy absorbed. In order to vary the power significantly by varying the hydrocarbon pressure, a wide range of pressures must be employed. The resulting variation in total pressure and in the ratio of reactants complicates the determination of power dependence. As expected, increasing the hydrocarbon pressure favors the production of nitrocycloalkanes, at least up to a point. When the cyclopropane pressure is varied, the nitrocyclopropane yield increases up to the cyclopropane pressure at which the nitrogen oxides reach a minimum: the nitrating agent is depleted; therefore, nitration ceases. In the cyclobutane pressure series, the nitrocyclobutane production also mirrors the nitrogen oxide use, although the nitrogen oxides do not absorb the CO₂ laser output directly, the nitrogen oxides pressure definitely has an impact on the cyclopropane reaction system. Increasing the nitrogen oxides pressure over the range studied has no discernible impact on the yield of vapor-phase nitrocyclopropane; however, the yields of some other products are dramatically increased by increasing the nitrogen oxides pressure, namely propene, acetonitrile, propenitrile, nitromethane and propenal. Therefore, the nitrogen oxides pressure must be strictly controlled at low levels to minimize the formation of side products.

Variation of the incident laser power over a limited range of powers allows the most direct access for determining power dependence. Instrumental limitations restricted us to 20–25 W cm⁻² as a minimum, below which lasing could not be sustained, and 100 W cm⁻² as a maximum for the strongest laser emissions. The CO₂ output lines available to directly irradiate the cyclic hydrocarbons are not the strongest and also correspond to weak hydrocarbon absorbances. Even so, we can extract some information about the dependence of nitrocycloalkane formation on incident power using data from the cyclopropane and cyclobutane experiments. Increasing the irradiation power favors the production of nitrocycloalkanes until that point when enough power is absorbed that fragmentation reactions dominate. A number of fragmentation products can be detected only after a certain threshold power and increase rapidly thereafter. There is, therefore,

a narrow range of powers that optimizes nitrocycloalkane production: the incident power must be high enough to support nitration but low enough to minimize excessive fragmentation.

Cyclopentane has even weaker absorption bands than do either cyclopropane or cyclobutane in the frequency range accessible through direct irradiation using the CO₂ laser. A sensitizer would help to overcome some of the limitations encountered in adjusting the laser output by providing a flexible, although indirect, means of varying power. The CO₂ laser has several emissions overlying an intense absorption region of SF₆, which also overlaps with a weak absorption band of cyclopentane. The frequency of irradiation can be varied so that SF₆ absorbs more or less of the energy. Alternatively, the pressure of SF₆ can be changed while keeping the ratio of nitrating agent to hydrocarbon constant and, at the low pressures of SF₆ required, keep the total pressure essentially constant. Varying the power with the aid of the sensitizer has an analogous effect to increasing incident power, that is, there is a narrow range of sensitizer pressures that favors nitrocyclopentane production and limits fragmentation. The most pronounced effect on fragmentation is observed when energy absorption is increased using a sensitizer.

Nitrocyclopentane formation is so favored, especially with SF₆ present, that the reaction cell becomes saturated with the vapor and the nitrocyclopentane begins condensing on the container walls. Using the cell-wash procedure, it was shown to be true for nitrocyclopentane, which has a vapor pressure of about 1 Torr, and it is possible that it can occur for the lower molecular weight nitroalkanes too, even though their vapor pressures are higher. Even at optimum pressures of SF₆ (1.0–1.5 Torr), nitrocyclopentane was the only nitroalkane detected in the condensed phase, evidence for the high selectivity of the laser-induced nitration process. The yield of nitrocyclopentane, based on the calibration graph, was 10–12% under optimum conditions, based on nitrogen oxides, the limiting reagent. Pure samples of nitrocyclopropane and nitrocyclobutane were unavailable for use as standards to determine their percentage yields. However, this 10–12% yield is better than the 3.6–5.0% yield [1] obtained in the thermal nitration of nitrocyclopropane. Because of the favorable yields in the cyclopentane reaction and the selectivity of the laser-induced nitration of the cyclic hydrocarbons, the possibility exists for a continuous process in which liquid nitrocycloalkanes can be recovered free of contamination.

With continued research in this area, these laser-induced nitrations could be driven to even higher yields. The lessons learned from the use of SF₆ with cyclopentane could be applied successfully to both cyclopropane and cyclobutane

and to other classes of compounds. As in the thermally driven, vapor-phase nitration [1] of cyclopropane, the laser-induced reaction of nitrogen with cycloalkanes is bimolecular in the case of all three compounds studied here. In all cases, there is indeed competing excitation-induced isomerizations of the cycloalkane to alkenes and resultant end product breakdown which is minimized by optimization. Similarly to the thermal vapor phase nitration of cyclopropane [1] above certain laser powers, both decomposition and oxidation occur, as indicated by the formation of alcohols. Longer processing times act similarly to high powers.

This laser-induced optimization research has yielded uniformly the optimal conditions for all three cycloalkanes. It is well known that optimal laser-induced processes can produce the maximum yield of a desired product while minimizing the formation of side products. This is very similar to process optimization thermally, particularly when using a sensitizer.

Acknowledgements

Judith M. Bonicamp, Susan E. Godbey and Larry M. Ludwick acknowledge financial support from the US Army Missile Command under Battelle Contract Number DAAL03-86-D-0001, in partial performance of this work. Appreciation is extended to Dr. S.P. McManus of the University of Alabama at Huntsville for providing the sample of cyclobutane.

References

- [1] H.B. Hass and H. Shechter, *J. Am. Chem. Soc.*, **75** (1953) 1382.
- [2] A.E. Stanley and S.E. Godbey, *Appl. Spectrosc.*, **43** (1989) 674.
- [3] A.E. Stanley, S.E. Godbey, J.M. Bonicamp and L.M. Ludwick, *Spectrochim. Acta, Part A*, **49** (1993) 1987.
- [4] A.E. Stanley, L.M. Ludwick, D. White, D.E. Andrews and S.E. Godbey, *Appl. Spectrosc.*, **46** (1992) 1866.
- [5] S.M. Khalit and H.M. Jarjis, *Z. Naturforsch.*, **46** (1991) 898.
- [6] Assa Lifshitz, Shock initiated pyrolysis of nitrocyclopropane, *Final Technical Report*, US European Research Office, London, 1966.
- [7] L.M. Sverdlov, M.A. Kovner and E.P. Krainov, *Vibrational Spectra of Polyatomic Molecules*, New York, 1974, and references cited therein.
- [8] D.C. Smith, C.-Y. Pan and J.R. Nielson, *J. Chem. Phys.*, **18** (1950) 706.
- [9] J.R. Durig, J.A. Smooter Smith, Y.S. Li and F.M. Wasac, *J. Mol. Struct.*, **99** (1983) 45.
- [10] G.T. Arakawa and A.H. Nielsen, *J. Mol. Spectrosc.*, **2** (1958) 413.
- [11] G.M. Begun and W.H. Fletcher, *J. Mol. Spectrosc.*, **4** (1960) 388.
- [12] J.R. Durig, F.Y. Sun, Y.S. Li and S.F. Bush, *J. Raman Spectrosc.*, **13** (1982) 290.
- [13] K.E. Gilkut and W.T. Borden, *J. Org. Chem.*, **44** (1979) 659.
- [14] R.H. Norton and R. Beer, *J. Opt. Soc. Am.*, **66** (1976) 259.